PARAMETRIC MICROWAVE HARMONIC GENERATOR

A Thesis

Presented to

The Faculty of Graduate Studies and Research

of the

University of Manitoba

In Partial Fulfillment

of the Requirements for the Degree

Master of Science in Electrical Engineering

by

Satish K. Vohra

April, 1968

ABSTRACT

A solid state (abrupt junction varactor) frequency doubler is designed to yield a stable output at 9.0 GHz. The varactor diode (BLV81EC with a cut-off frequency of 60 GHz) was mounted at the centre of a crossed waveguide structure which includes a number of matching and tuning devices. The experimental arrangement of the waveguide assembly and the technique of diode mounting together with measurements made on this doubler is discussed. The conversion efficiency and the basic operation of the harmonic generator are presented from an idealized equivalent circuit model. It is shown that for the frequency doubler 4.5 to 9.0 GHz the measured power efficiency is approximately 56% without taking the attenuation loss of the bandpass filter into account and is 38% when this loss is taken into account. Much higher efficiency than reported here is realizable with the use of the relatively new step recovery diode.

ACKNOWLEDGEMENT

The author wishes to acknowledge the assistance and guidance given by Professor M. A. K. Hamid throughout the project.

Sincere thanks are also due to Dr. J. W. Bandler for many hours of discussions. The author also wishes to thank Mr. R. Woods and Mr. H. Unger for their excellent machine work and to Miss L. M. Walker for the excellent typing of the manuscript.

The financial assistance of the National Research Council of Canada, in the form of Grant A-3326, is also acknowledged.

TABLE OF CONTENTS

TABLE OF CONTENTS (continued)

TABLE OF CONTENTS (continued)

LIST OF FIGURES

LIST OF FIGURES (continued)

CHAPTER I

INTRODUCTION

Efficient harmonic generators are presently used as convenient sources of microwave power at millimeter and submillimeter wavelengths [1,2]. Their use has also been recently extended to generate standard frequencies in microwave laboratories by multiplying the output of a crystal stabilized oscillator.

1.1 FREQUENCY AND POWER LIMITATIONS OF MICROWAVE SOURCES:

In spite of many attempts, there has as yet been very limited success in producing coherent electromagnetic radiation at the millimeter and submillimeter wavelengths. Only one type of conventional microwave tube, the CSF* carcinotron, has been reported to operate successfully at millimeter wavelengths. About 10 milliwatts of power has been generated by this experimental tube [3,4]. This achievement represents remarkable progress in the scaling down of a conventional microwave tube. There are, however, certain fundamental limitations outlined by Pierce [5] in 1950, which makes it extremely difficult, if not impossible, to achieve the operation of conventional tubes at very high frequencies.

The physical dimensions of the interaction region within the tube are generally a fraction of a wavelength so that precise construction of components becomes very difficult at shorter wavelengths. Furthermore,

---

*Manufactured by Compangie Generale de Telegraphie Sans Fil, Paris, France.

losses increase with frequency thus lowering the tube efficiency and increasing the heat that must be dissipated. The physically smaller size, on the other hand, makes heat dissipation more difficult and, consequently, limits the input power that can be used to get appreciable interaction between the electron beam and the electromagnetic fields. It is necessary to have increasingly higher current densities as the frequency is increased. Space charge effects seriously limit the maximum electron density that can be achieved in an electron beam, while the attainable cathode current density also presents a limitation for microwave tubes. In all of the conventional tube types, these factors combine to make oscillations in the shorter wavelength region either impossible, or with such high losses, that only a small amount of r.f. energy can be generated.

The maximum continuous power available from microwave tubes is shown in Figure 1*. In the range from 10 GHz to 300 GHz, the available power falls at the rate of about 40 dB per decade (12 dB per octave). With the exception of CSF as already mentioned, operation at higher frequencies has not yet been achieved. The success of the CSF tube shows how far conventional tube techniques can be extended. The lack of progress in extending other tube types, both in power and frequency, is related to the expense of conducting such research, and the very limited demand for these tubes.

Consider some of the other methods for producing microwave energy. Coherent electromagnetic power, both cw and pulsed, has been produced at optical wavelengths by masers or lasers [6]. At present, however, maser

*This data has been collected from different commercial tubes available for producing microwave energy.

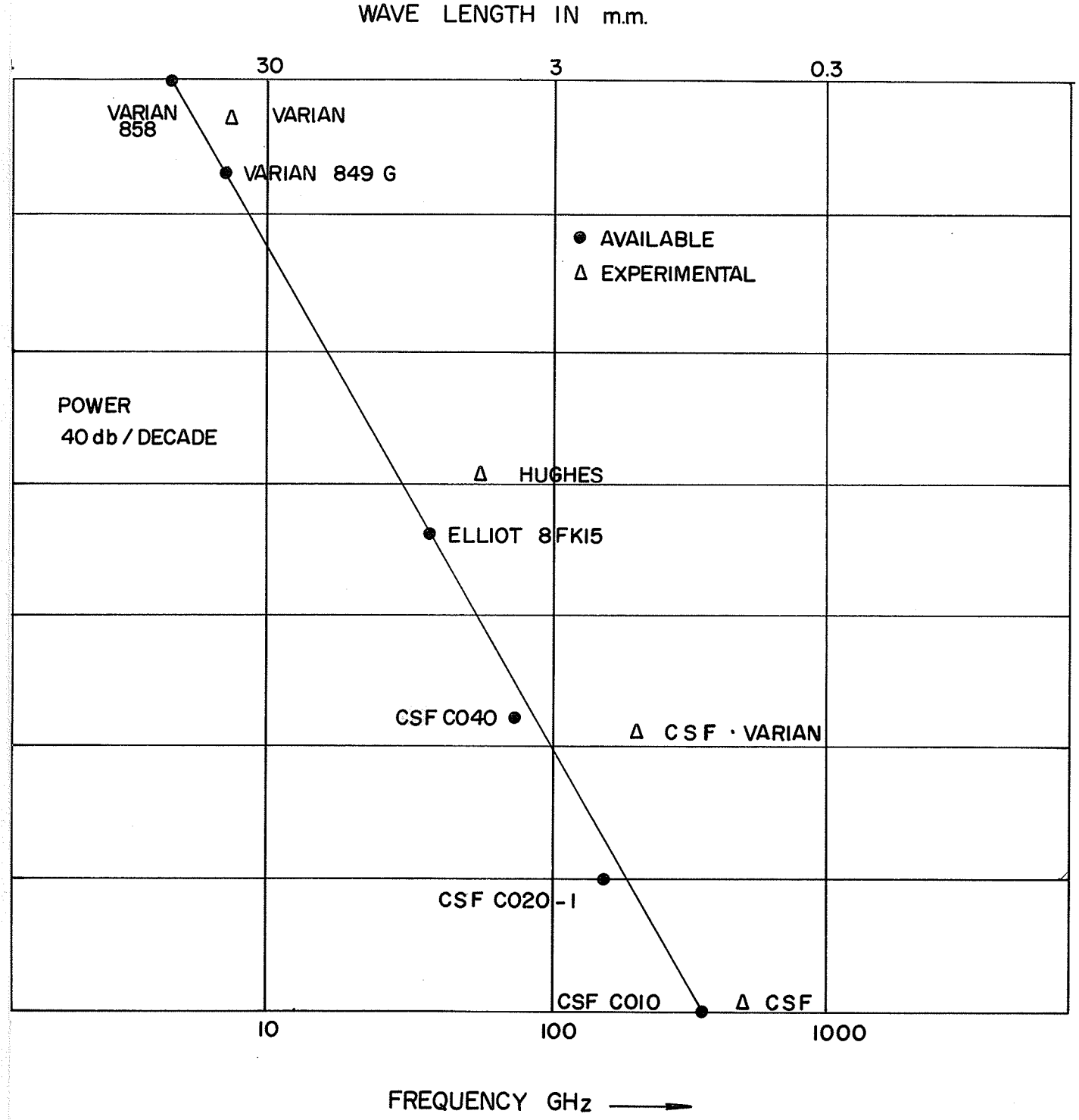
WAVE LENGTH IN m.m.
30
3
0.3
VARIAN 858
Δ VARIAN
VARIAN 849 G
● AVAILABLE
Δ EXPERIMENTAL
POWER
40 db / DECADE
Δ HUGHES
ELLIOT 8FK15
CSF C040
Δ CSF · VARIAN
CSF C020-1
CSF C010
Δ CSF
10
100
1000
FREQUENCY GHz

FIGURE. 1.

oscillators and amplifiers are not available in the wavelength region below 10 millimeter. One difficulty here might be due to the lack of information about suitable transitions resulting from the very limited work in spectroscopy at these wavelengths. The highest microwave frequency yet produced coherently was obtained by an "arc harmonic generator" developed by Froome* in England. Using 5 watts of continuous wave power at 35 GHz, harmonics as high as the 21st (735 GHz) have been detected. P-N junction diodes for a long time have been used in frequency multipliers [7]. But, Page [8] has shown that the efficiency (power output/power input) for a frequency multiplier employing ideal non-linear resistance diodes is limited to $1/N^2$, where N is the harmonic number of interest. The reason for low efficiency is due to high resistive losses presented by these devices.

1.2 HARMONIC GENERATION BY NON-LINEAR REACTANCE DEVICES:

A power gain can be obtained if a variable resistance device is replaced by a variable reactance device. A basic description of the mechanism for harmonic generation by non-linear reactance is given by the fundamental power relations developed by Manley and Rowe [9]. These equations state in effect, that all the power applied to a lossless non-linear reactance device at one or more arbitrary frequencies, must emerge as an equal power at harmonics of the driving frequency, i.e. 100% conversion efficiency is possible. In practice, however, such an ideal device can only be approached. Semiconductor "varactor" diodes (variable capacitance diodes), due to their low loss properties, come nearest to

---

*See Reference [7]

satisfying this ideal condition and can therefore be used for efficient microwave harmonic generation and amplification. A varactor [10, 11] is a diffused p-n junction semiconducting device with non-linear voltage-charge characteristics and is normally operated in the reverse-bias region. The most important distinction between varactors and conventional diodes, is that the varactor exhibits much lower parasitic-resistive losses, thus enabling efficient power conversion. Moreover, variable reactance devices have proved their superiority over other devices with regard to low noise characteristics [12, 13, 14].

In the present investigation the theory and use of the varactor diodes for frequency multiplication is discussed in Chapter II and the theory of harmonic generation is reviewed briefly in Chapter III. The conversion efficiency of the harmonic generator is predicted theoretically in Appendix B while the multiplier design and the experimental results are presented in Chapter IV. A conversion efficiency of about 40% has been obtained for 4.5 GHz to 9.0 GHz harmonic generator. The comparison between the theory and experiment is discussed in Chapter V.

CHAPTER II

THE THEORY AND APPLICATIONS OF THE VARACTOR DIODE

2.1 THE PHYSICAL STRUCTURE OF THE DIODE:

The varactor is a p-n junction semiconductor device having a non-linear charge-voltage characteristic. Its junction capacitance can be varied by varying the reverse bias. All p-n junctions exhibit non-linear barrier capacitance; if this effect predominates in some sense, then the junction can be used to advantage as a varactor diode. Excellent discussions of p-n junctions and junction capacitance are presented in the literature [15, 16, 17]. Instead of giving a rigorous treatment here we present sufficient background material for discussion of junction capacitance.

It is a well known fact that a p-n semiconductor junction acts as a rectifier, passing current in only one direction. For a simplified picture, suppose a battery is connected to the ends of a semiconductor, with its positive terminal to the p-region. The energy level diagram for this configuration is shown in Figure (2.1c). As a consequence, the junction-barrier potential is reduced to $q(V_J - V_F)$ and there is a net flow of current across the junction and through the external circuit. The current consists of holes which are injected from the P-region into the n-region and of a flow in the opposite direction of injected electrons. On the other hand, if the battery is reversed, the barrier potential is increased to $q(V_J + V_R)$ as shown in the Figure (2.1b). The carriers of

each type would be drawn back away from the junction and no net current would flow except the saturation current due to minority carriers.

2.1.1 The Variable Capacitance Property:

In the absence of external bias across the diode, equilibrium is established between the two regions as shown in Figure (2.1a) resulting in the same Fermi level for the two regions. A narrow region is left at the junction which is free of carriers. This region is called the depletion layer and acts as a parallel plate capacitor separated by two conductive regions. It can be seen that by increasing the junction voltage V_J by means of reverse bias as shown in Figure (2.1b), it will increase the thickness of the depletion layer. This occurs because electrons and the hole distribution will be pulled in the opposite direction so that the net distance between the two barriers is increased. As the depletion layer width increases, the junction capacity decreases. On the other hand, when forward bias is applied as shown in Figure (2.1c), the two barriers will be pushed forward and the width of the depletion layer decreases. Thus capacitance may be varied by changing the external bias.

The precise dependence of the junction capacitance upon the applied voltage varies with the nature of the junction. In abrupt junctions, where n-type doping changes to p-type doping in an abrupt step, the capacitance is inversely proportional to the square root of the applied voltage*. In graded junctions, i.e. where doping changes gradually from n-type to p-type, the capacitance varies more like the reciprocal cubic root of the applied voltage. These cases are shown in

*See Appendix A, equation (A.3)

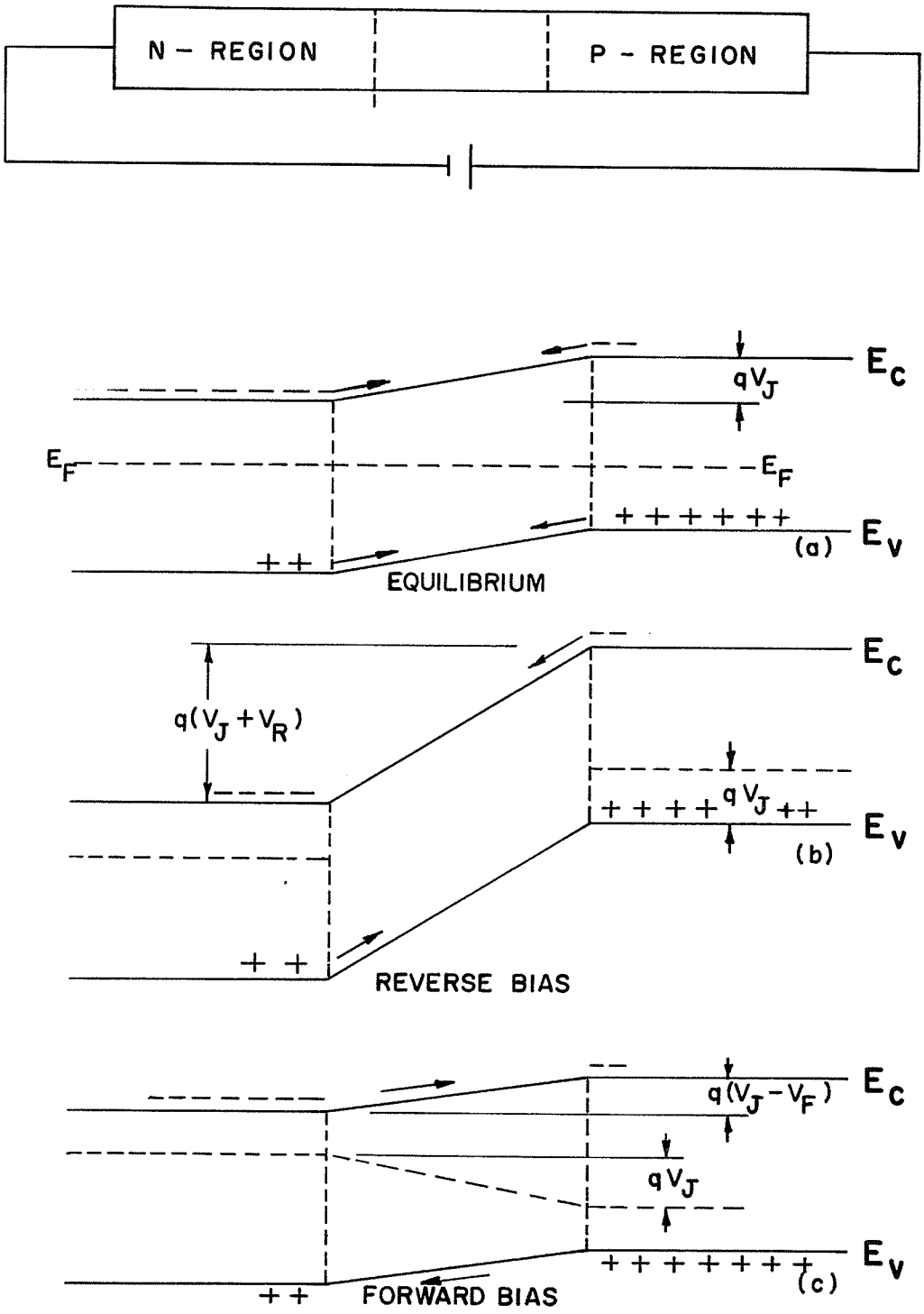

FIGURE 2.1

ENERGY LEVEL DIAGRAM FOR THE DIODE

Figures (2.2a) and (2.2b) where $N(X)$ represents the doping density and positive X is the distance measured away from the junction into the n-region.

2.2 THE EQUIVALENT CIRCUIT:

There are three physical effects that should be included in the varactor equivalent circuit. These are the non-linear junction capacitance, the series resistance R_s and the conduction across the junction. We represent the junction conduction, approximately by a non-linear conductance $G(V)$* where V is the instantaneous voltage across the junction. Besides these three parameters, we should include in the equivalent circuit any inductance L_{lead} of the wires leading to the semiconductor and any stray capacitance C_{case} of the package enclosing the varactor. The resulting equivalent circuit is shown in Figure (2.2c).

The above equivalent circuit may be simplified in the following manner. The conductance $G(V)$ may be neglected since in high quality varactors it is effectively shunted by $C(V)$. L_{lead} and C_{case} may also be neglected in high quality varactors at high frequencies, since their contribution to the final behaviour of the circuit is negligible. The simplified resulting circuit [18] is also shown in Figure (2.2c).

2.3 THE CUTOFF FREQUENCY, CONTACT POTENTIAL AND NORMALIZED POWER:

Cutoff frequency is the characterization of the varactor quality and is defined as:

$$\omega_c = \frac{S_{max} - S_{min}}{R_s}$$

---

*Please see Reference [46].

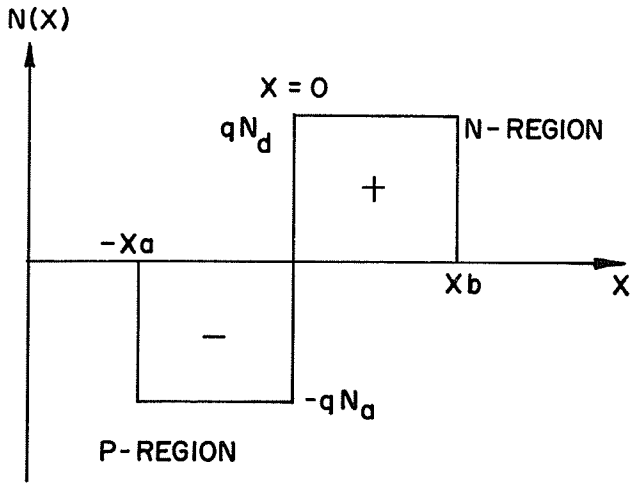

ABRUPT JUNCTION

(a)

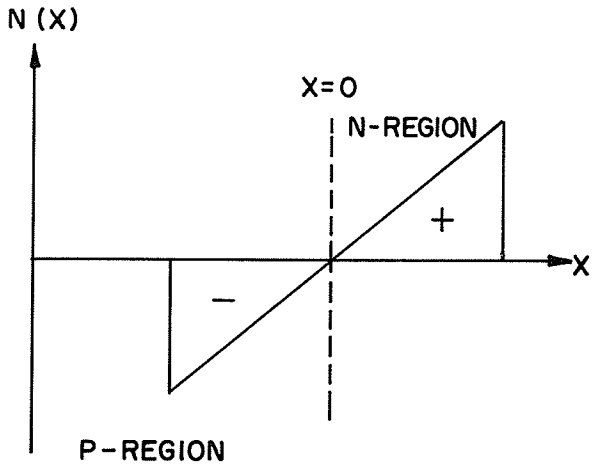

GRADED JUNCTION

(b)

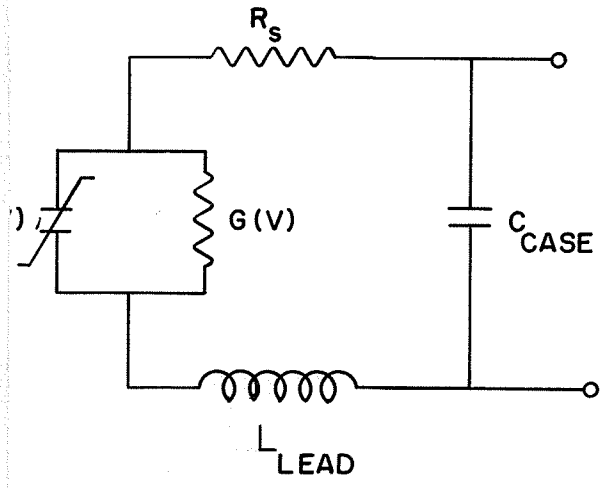

(c)

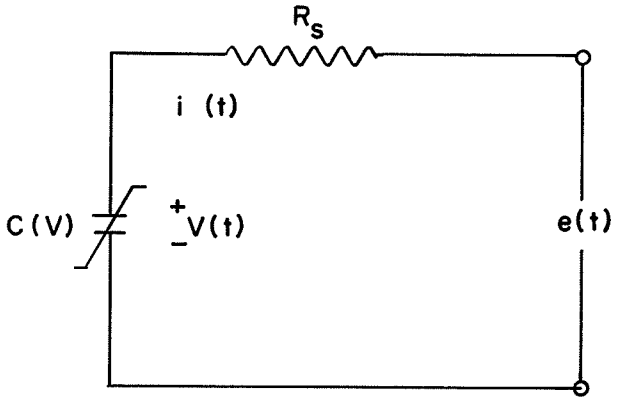

SIMPLIFIED CIRCUIT

EQUIVALENT CIRCUIT OF VARACTOR DIODE

FIGURE (2.2)

where S_{max} (or C_{min}) is the maximum elastance (or minimum capacitance) occurring at breakdown voltage. S_{min} is the non-zero value* of elastance at a voltage $V = V_{min}$. The above definition for cutoff frequency becomes identical to that proposed by Uhlir in 1958 [18], for negligibly small S_{min}. Hence

$$f_c = \frac{1}{2\pi R_s C_{min}} \qquad (2.2)$$

we can see that the cutoff frequency of the varactor is virtually limited by R_s, the series resistance of the diode.

Contact potential is due to the incomplete compensation between the fixed charge density and mobile charges. For p-n junctions, this voltage ranges between 0.1 to 0.5 volt. It is more convenient to express the non-linear element in terms of an incremental elastance S(V) instead of an incremental capacitance C(V) i.e.

$$S = \frac{1}{C} = \frac{\Delta V}{\Delta q}$$

For an abrupt junction varactor, the elastance, the contact potential, and applied voltage are related by:

---

*As V approaches ϕ in the forward conduction region (Figure 2.3), (2.5) is only approximate, since the nonlinearity changes in this region. Also, the edge of the depletion layer is not flat to the extent that $S = 0$ at $V = \phi$. In practice, S approaches a non-zero value S_{min}, at a voltage $V = V_{min}$.

$$S(V) = S_{max}\left[\frac{V + \phi}{V_B + \phi}\right]^{\frac{1}{2}} \qquad (2.4)$$

where S_{max} is maximum elastance at breakdown voltage V_B and ϕ is the contact potential. For graded junction varactors, the corresponding expression [19] is given by:

$$S(V) = S_{max}\left[\frac{V + \phi}{V_B + \phi}\right]^{1/3} \qquad (2.5)$$

Normalized power of a varactor diode is a measure of its power handling capabilities and is given by:

$$P_{norm} = \frac{(V_B + \phi)^2}{R_s} \qquad (2.6)$$

The higher the normalized power (for a given cutoff frequency), the higher the power levels that the varactor is inherently capable of handling. A related quantity which gives a more specific indication of power handling capability at a particular frequency is the nominal reactive power as used by Uhlir [18, 41]:

$$P_r \simeq C_{min} V_B^2 \frac{f_{in}}{2} \qquad (2.7)$$

It can be shown [19] that, to a good approximation, the maximum input power P_{in} which can be efficiently transformed to harmonic power can be given, for the abrupt junction, by the equation

$$P_{in} = 0.2\, f_{in}\, C_{min}\, (V_D - V_B)^2 \qquad (2.8)$$

where f_{in} is the input frequency, V_D is the diffusion voltage and C_{min} is the capacitance at breakdown voltage V_B.

2.4 THE ELECTRIC CHARACTERISTICS

The V-I characteristic of a typical diode is shown in Figure (2.3a). The reverse current is nearly constant to quite a high negative bias. Eventually, a critical voltage $-|V_B|$ is reached beyond which the current increases rapidly. This voltage is usually referred to as the avalanche (breakdown) voltage. The large increase in current is due to impact ionization. The non-linear capacitive voltage characteristic is shown in Figure (2.3b). The capacitance assumes a minimum value C_{min} at the breakdown voltage V_B. In figure (2.3c), the elastance has been plotted as a function of the applied voltage for an abrupt-junction varactor diode according to the equation (2.4). It can be noted that maximum elastance is achieved at the reverse breakdown voltage V_B.

2.5 APPLICATIONS

Since the series resistance of a varactor diode is very small and the quality factor Q (or $\frac{1}{\omega C R_s}$) is large, the power losses of the device are relatively small making it attractive for use in high frequency multipliers, amplifiers, mixers, detectors [1], and sub-harmonic generators. The junction is very thin because of its heavy doped p-n semiconducting materials, and therefore the diode can be used as a good switching device

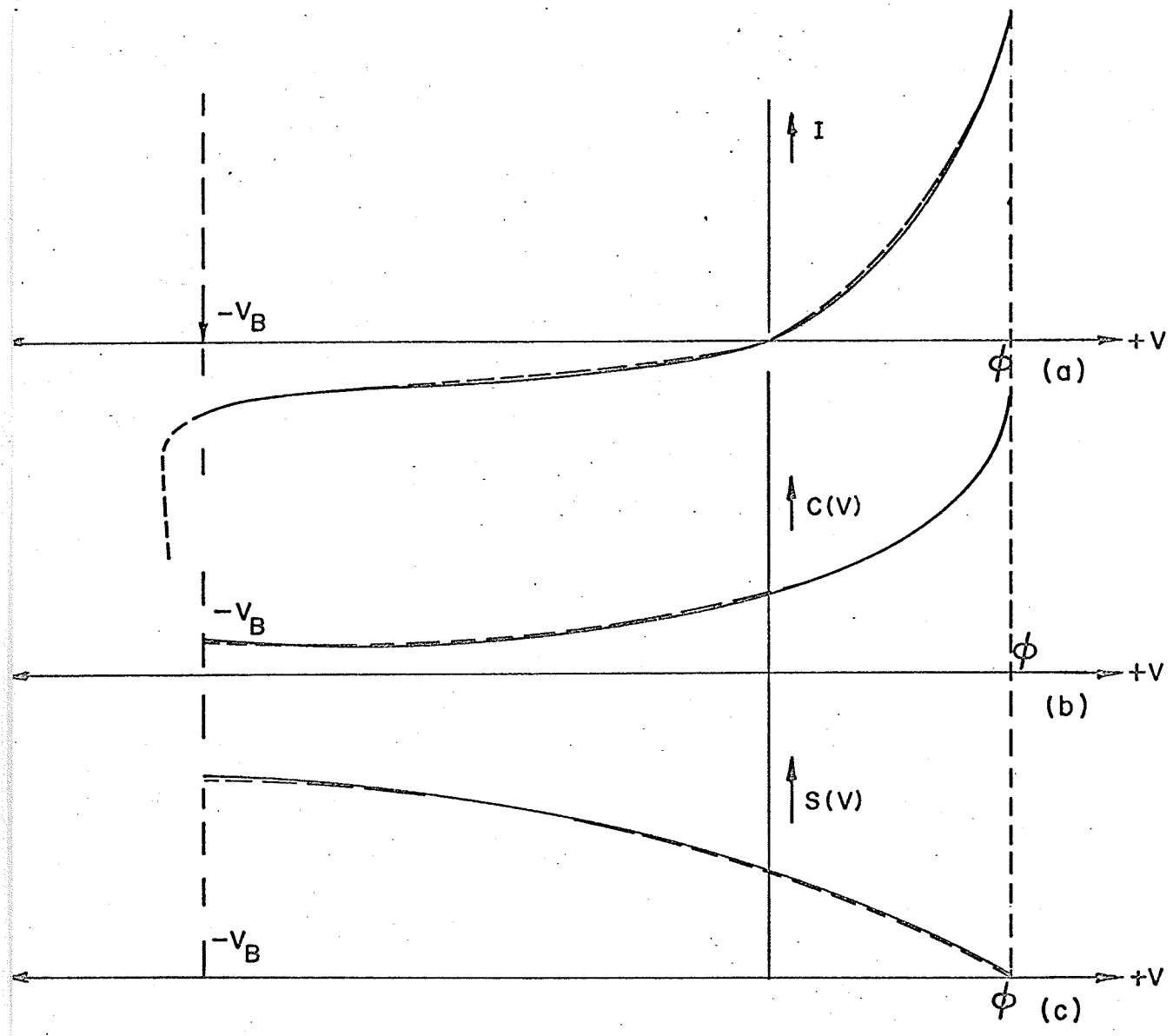

ELECTRIC CHARACTERISTICS OF "VARACTER"

(a) VOLT – AMP CURVE

(b) CAPACITANCE – VOLTAGE CURVE

(c) ELASTANCE – VOLTAGE CURVE

FIGURE (2.3)

e.g. in high speed computers [20].

The simplest application for the diode is for harmonic generation or frequency multiplication [21, 22, 23]. The varactor is excited at a frequency f_o and power is delivered to the load at frequency $2f_o$, $3f_o$, or in general, nf_o where n is a positive integer. A chain of varactor multipliers, driven by v.h.f. transistor amplifiers, makes a very practical solid state source of microwave power.

Another application is for frequency division or subharmonic generation [24]. If the varactor is excited at f_o, power may be delivered to a load at $f_o/2$, $f_o/3$ or in general f_o/n.

An additional application is in frequency convertors when a large current at a frequency f_p and a small current at a frequency f_s are put through a varactor, side bands with frequencies $(n f_p + f_s)$ are generated. If the output frequency is greater than f_s it is an upconverter, otherwise it is a downconverter [25].

Another importance application is in parametric amplifiers [26]. The varactor is pumped at a frequency f_p and a signal is introduced at a frequency f_s. If the varactor is properly terminated at the side band $(f_p - f_s)$, then the varactor behaves at f_s as if it were an impedance with negative real part. This negative resistance is responsible for the mechanism of amplification.

2.6 THE DESIGN OF VARACTOR DIODES FOR FREQUENCY MULTIPLIERS*

2.6.1 The Design Criterion for Varactor Diodes.

The design of the varactor diode is governed by three requirements imposed by (1) the circuit; (2) the semi-conductor materials; and (3) the processing and fabrication technology. For example, a switching diode may be quite different from a diode for communication use. Diodes for low frequency and low speed are easier to realize than those for very high frequencies and speed. The varactor diode for harmonic generation should have a high cutoff frequency. This requires a low series resistance and a low diode capacitance, which are difficult to achieve simultaneously. Impurity doping is an important parameter because it controls the barrier capacitance and series resistance and hence, the cutoff frequency. A high cutoff frequency requires a low resistance and thus material with high mobility. InSb and InAs have the highest mobilities, but they have to be operated at low temperatures. High cutoff frequency (i.e. reduced R_s) can be obtained through the use of recently developed pulsed formed p-n junctions. The junction and the forming technique is that proposed by Burrus [27]. The best results to date, in both power handling capability and efficiency, have been obtained with GaAs varactor diodes. The diode made on this material had very sharp reverse breakdown voltage in the range of 15 to 20 volts. A conversion efficiency of 20% has been obtained by using these diodes for a 70 to 140 GHz harmonic generator [2].

---

* For a complete analysis and the predicted conversion efficiency, the reader is referred to Appendix B.

2.6.2 A Hypothetical Design of a Varactor for a Frequency Doubler

As a hypothetical case, we assume the following design parameters:

Signal frequency = 4.5 GHz

Input power P_{in} = 100 m watts (desired)

Dissipation P_{diss} = 35 m watts (allowed)

Therefore Efficiency = $\frac{50 \times 17.5 \times 100}{50}$ = 65%

From the curves of $\frac{\omega_c}{\omega_o}$ vs Conversion Efficiency*

we obtain:

$$\frac{f_c}{f_o} = 14$$

hence

$$f_c = 63 \text{ GHz}$$

From another curve of $\frac{f_{in}}{f_c}$ vs P_{in} given in Appendix B we obtain:

$$\frac{P_{in}}{P_{norm}} = 5 \times 10^{-3}$$

$$\frac{100 \times 10^{-3}}{P_{normal}} = 5 \times 10^{-3}$$

hence

$$P_{norm} = 20 \text{ watts}$$

But

$$P_{norm} = \frac{(V_B + \phi)^2}{R_s} = 20$$

---

* See Appendix B, equations (B.30) to (B.32).

Assuming V_B the breakdown voltage equals 10 volts and ϕ the contact potential = 0.5 volt then,

$$\frac{(10.5)^2}{R_s} = 20$$

hence

$$R_s = \underline{5.2 \text{ ohms}}$$

Now

$$f_c = \frac{1}{2 \pi R_s C_{min}}$$

Therefore $$C_{min} = \frac{1}{2 \pi f_c R_s}$$

$$= \frac{1}{2 \times 3.14 \times 63 \times 5.2} \times 10^{-9} \simeq 0.1 \text{ pf}$$

hence the parameters of this diode are

Cutoff frequency = 60 GHz

Breakdown voltage = 10volts

Series resistance = 5.2 ohms

Capacitance at breakdown = 0.1 pf.

Diodes having such characteristics are commercially available and alternatively, are simple to construct with reasonable facilities.

CHAPTER III

HARMONIC GENERATOR (DOUBLER)

3.1 PRINCIPLE OF HARMONIC GENERATION:

A harmonic generator, in principle, multiplies power at one frequency to the power at another frequency. In this thesis we are interested in the use of a varactor diode as the non-linear element for microwave harmonic generation. The use of a varactor diode as a microwave semiconducting device is due to the non-linear charge vs voltage characteristics of a p-n junction operating in the reverse bias region as shown in Figure (3.1). The resultant voltage wave is seen to be strongly distorted and rich in harmonics. With the aid of proper filters and impedance matching devices, the harmonic frequency of interest is extracted from the distorted voltage signal. The percentage of fundamental power which is transferred to the harmonic frequency of interest is defined as the conversion efficiency. Conversion efficiency of 100% can be obtained by having perfectly matched devices and infinite Q varactor diodes. However, less efficiency is obtained under practical conditions.

Page [8] has studied the harmonic generation with non-linear resistor diodes and obtained a theoretical efficiency of $\frac{1}{N^2}$, where N is the harmonic number. Since a varactor diode is essentially a non-linear reactance with no power dissipated theoretically, its efficiency is therefore expected to be higher than for lossy non-linear devices. The

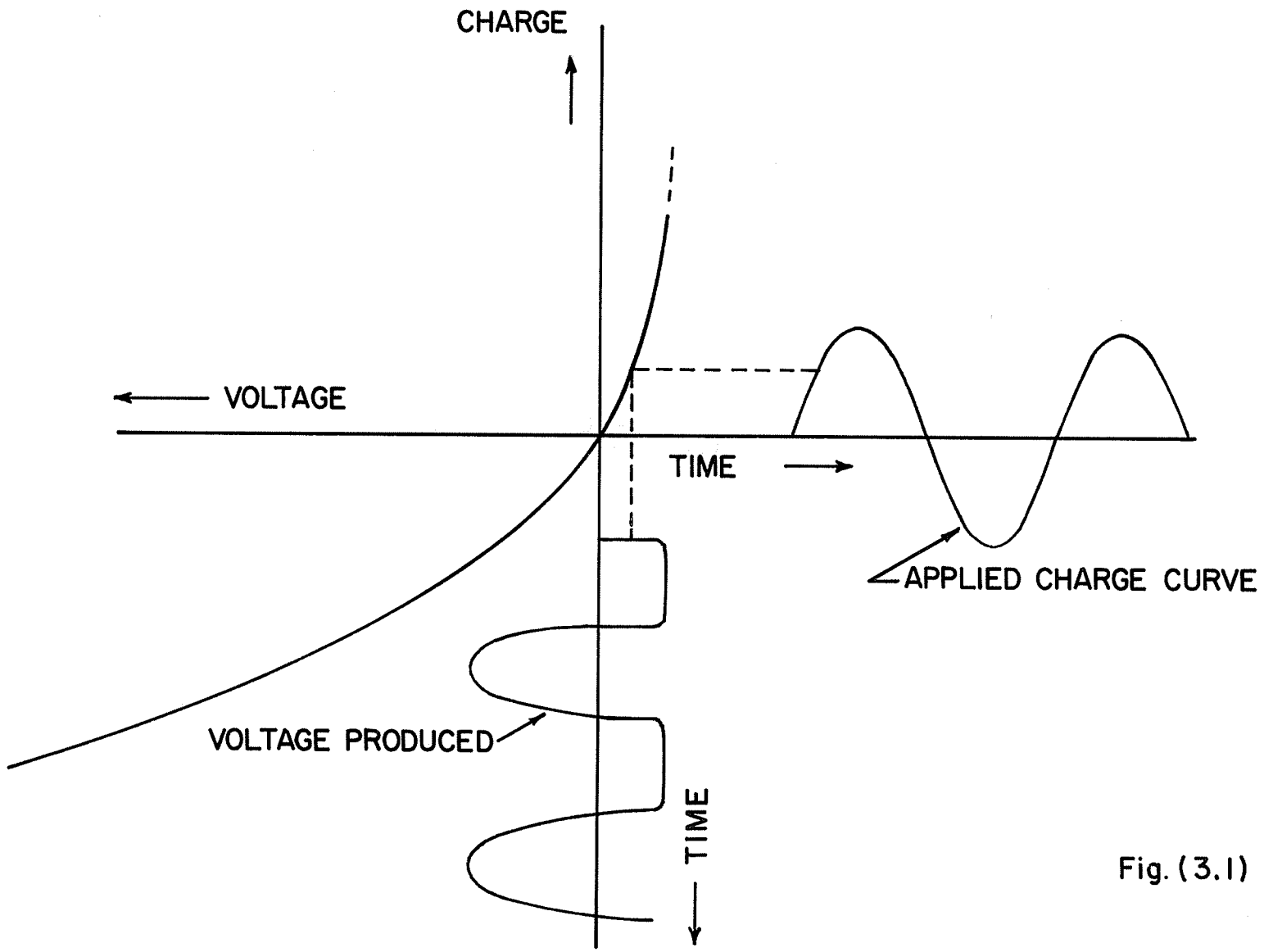
CHARGE
VOLTAGE
TIME
APPLIED CHARGE CURVE
VOLTAGE PRODUCED
TIME

Fig. (3.1)

additional advantage of higher power handling capacity, higher cutoff frequency and high S/N ratio makes the varactor diode a more promising device in efficient generation of millimeter waves.

3.2 MANLEY-ROWE POWER RELATIONS:

In order to predict the power efficiency of a non-linear reactance device, we make use of the Manley-Rowe power relations [9]. These authors have derived a very general set of equations relating power flowing into and out of an ideal non-linear reactance. These relations are a powerful tool in predicting whether power gain is possible in a given situation and the maximum gain that can be achieved.

Consider a non-linear capacitor excited with two frequencies f_1 and f_o (or ω_1 and ω_o) together with series resistances and band-pass filters as shown in the Figure (3.2). These filters are tuned to various sum and difference frequencies and are designed to reject the power at all frequencies other than their respective signal frequencies. Positive and negative sign conventions are used for power flowing into and out from the non-linear capacitance, respectively. Because of the non-linearity, side bands with frequencies of the form $m\omega_1 + n\omega_o$ for positive and negative integral values of m and n are generated.

In general the non-linear capacitor exchanges power with its terminations at all generated side bands where voltage $V(t)$ across the capacitor and the current $i(t)$ through it (see Fig. 2.2c) may each be expanded in a Fourier series [39].

$$V(t) = \sum_{m=-\infty}^{+\infty} \sum_{n=-\infty}^{+\infty} V_{mn}\, e^{j(m\omega_1 + n\omega_o)t} \qquad (3.1)$$

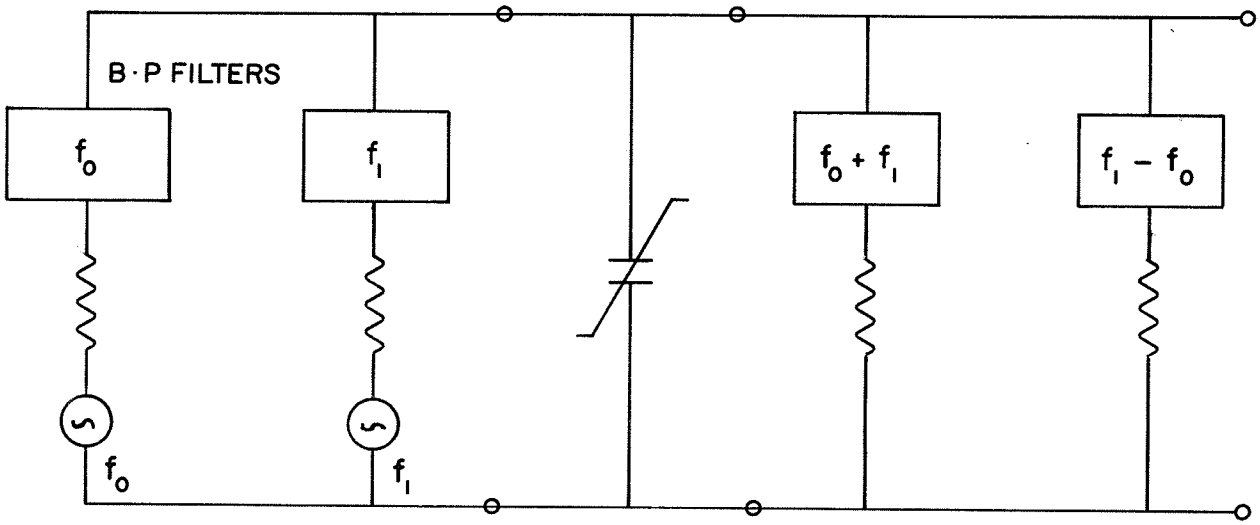

CIRCUIT MODEL FOR MANLEY - ROWE DERIVATION

FIGURE (3.2)

$$I(t) = \sum_{m=-\infty}^{\infty} \sum_{n=-\infty}^{\infty} I_{mn} e^{j(m\omega_1 + n\omega_o)t} \tag{3.2}$$

The time averaged power delivered to the non-linear capacitor is zero, because the capacitor, although non-linear, is lossless. However, the effect of non-linearity is the conversion of power from one frequency to another.

Let P_{mn} be the power into the capacitor at frequency $(m\omega_1 + n\omega_o)$ where

$$P_{mn} = 2 \text{ Re } [V_{m,n} I^*_{mn}] \tag{3.3}$$

Then the fact that the capacitor is lossless is expressed by

$$\sum_{mn} P_{mn} = 0 \tag{3.4}$$

where the summation extends over all combinations of m and n such that $m\omega_1 + m\omega_o$ is positive.† The Manley-Rowe formulas are

$$\sum_{m=0}^{\infty} \sum_{n=-\infty}^{+\infty} \frac{m P_{mn}}{m\omega_1 + n\omega_o} = 0 \tag{3.5}$$

---

† The sum can be over, instead, any combination of m and n such that only one pair of frequencies $(m\omega_1 + n\omega_o)$ and $-(m\omega_1 + n\omega_o)$ is included for each m and n. For example, we may sum m from $-\infty$ to $+\infty$, n from 0 to ∞.

$$\sum_{n=o}^{\infty} \sum_{m=-\infty}^{+\infty} \frac{n P_{mn}}{m\omega_1 + n\omega_o} = 0 \qquad (3.6)$$

3.2.1 Application of the Manley-Rowe Relations.

The usefulness of the Manley-Rowe power relations can be illustrated by several cases in which power flow at only three frequencies is allowed. By giving integer values for m and n, e.g. $m = 1$ and $n = 1$, there are three frequencies, f_o, f_1 and $f_o + f_1$. f_o is the signal source frequency and f_1 is the so called pump source frequency

Consider first the case where power flow is allowed at a frequency f_2 which is the sum of f_o and f_1. The powers at these frequencies are assumed to be P_o, P_1 and P_2 respectively. The Manley-Rowe relations lead to the expressions:

$$\frac{P_o}{f_o} + \frac{P_2}{f_o+f_1} = 0 \quad \text{or} \quad \frac{P_o}{f_o} + \frac{P_2}{f_2} = 0 \qquad (3.7)$$

$$\frac{P_1}{f_1} + \frac{P_2}{f_o+f_1} = 0 \quad \text{or} \quad \frac{P_1}{f_1} + \frac{P_2}{f_2} = 0 \qquad (3.8)$$

In equation (3.7) energy is supplied to the non-linear reactance at f_o while P_o is positive and P_2 is negative. This indicates that power flows from the reactance to the load at frequency f_2. Then the power gain can be defined as:

$$\text{gain}_{0-2} = -\frac{P_2}{P_o} = \frac{f_2}{f_o} \qquad (3.9)$$

We see this is the first example of the so called up-converter which provides a power gain equal to the ratio of the output to input frequencies. This corresponds to maximum theoretical gain.

As a second example, let the signal frequency be the sum of the pump frequency f_1 and the output frequency f_2. Thus $f_2 = f_o - f_1$ and $m = 1$ and $n = -1$. In this case the $\text{gain}_{2-0} = \frac{f_o}{f_2}$ which is the loss in the so called down converter [25].

As a third example let the power flow at a frequency equal to the difference between the pump and the signal. That is, let f_o be the signal frequency, f_1 the output frequency, and f_2 the pump frequency, with $f_o + f_1 = f_2$. Here we are supplying power at f_2 hence P_2 is positive while P_o and P_1 are negative. As already explained in Chapter II the varactor behaves at f_o as if it were an impedance with negative real part and therefore delivers power to the signal generator. If we define the gain as the ratio of the power supplied to the generator at f_o (by the non-linear reactance) to that supplied by the signal generator itself, then infinite gain is possible, because the reactance can deliver power at f_o whether a signal generator at f_o is delivering power or not. That is, the Manley-Rowe relations predict that such a device is potentially unstable and is capable of oscillations. This is another example of a parametric device often called a negative resistance parametric amplifier [26].

The last important device is so called the harmonic generator [21, 22, 23]. By allowing only two frequencies to exist and letting $m = 0$ and $n =$ any single integer, we have from the

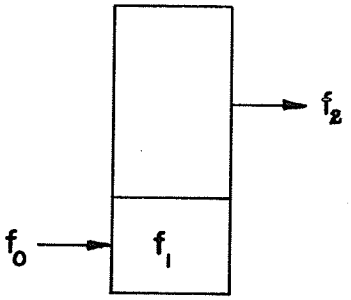

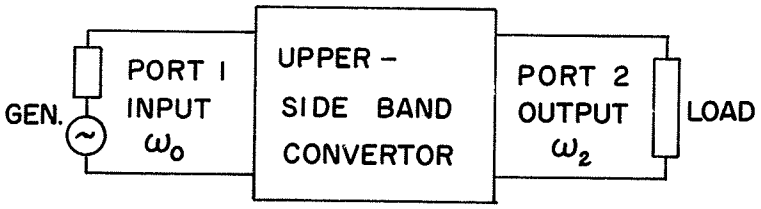

$f_2 = f_0 + f_1$

UPCONVERTOR

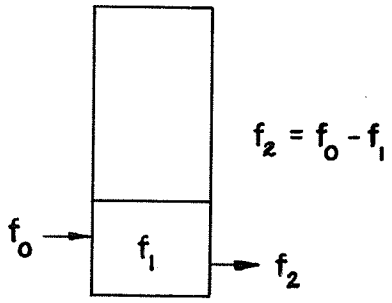

DOWNCONVERTER

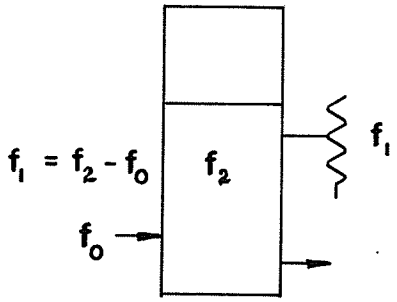

PARAMETRIC AMPLIFIER

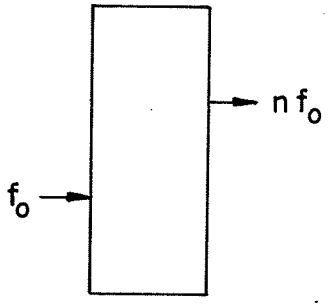

HARMONIC MULTIPLIER

FIGURE (3.3)

Manley-Rowe relations

$$\frac{P_o}{f_o} + \frac{n\,P_n}{n\,f_o} = 0$$

P_o = power flow in at f_o

P_n = power flow out at $n\,f_o$.

The efficiency is then given by

$$\frac{P_n}{P_o} = -1$$

which indicates a conversion efficiency of 100%, regardless of the order of the harmonic involved. In practice the actual efficiency is less than 100% due to:

(a) losses in the circuit element,

(b) loss in the series resistance of varactor diode,

(c) small but finite amount of power dissipated at harmonics other than the desired output frequency.

3.3 BASIC CIRCUITS FOR THE FREQUENCY DOUBLER:

There are two basic circuits from which a second harmonic can be obtained. Their operation depends upon whether the varactor diode is in series or in parallel with the transmitting system. They are classified as follows:

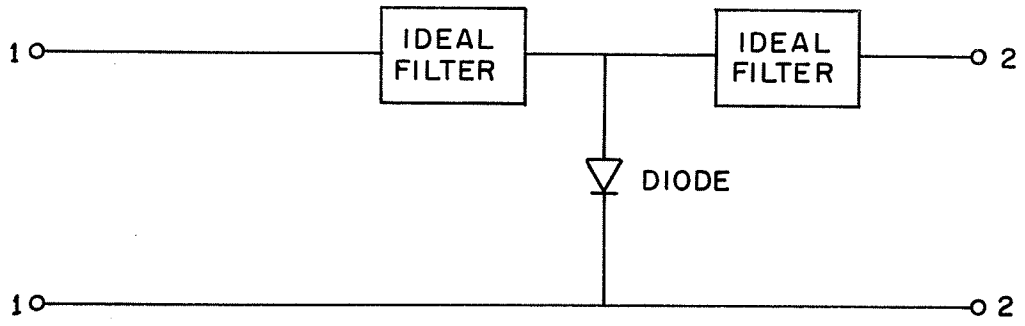

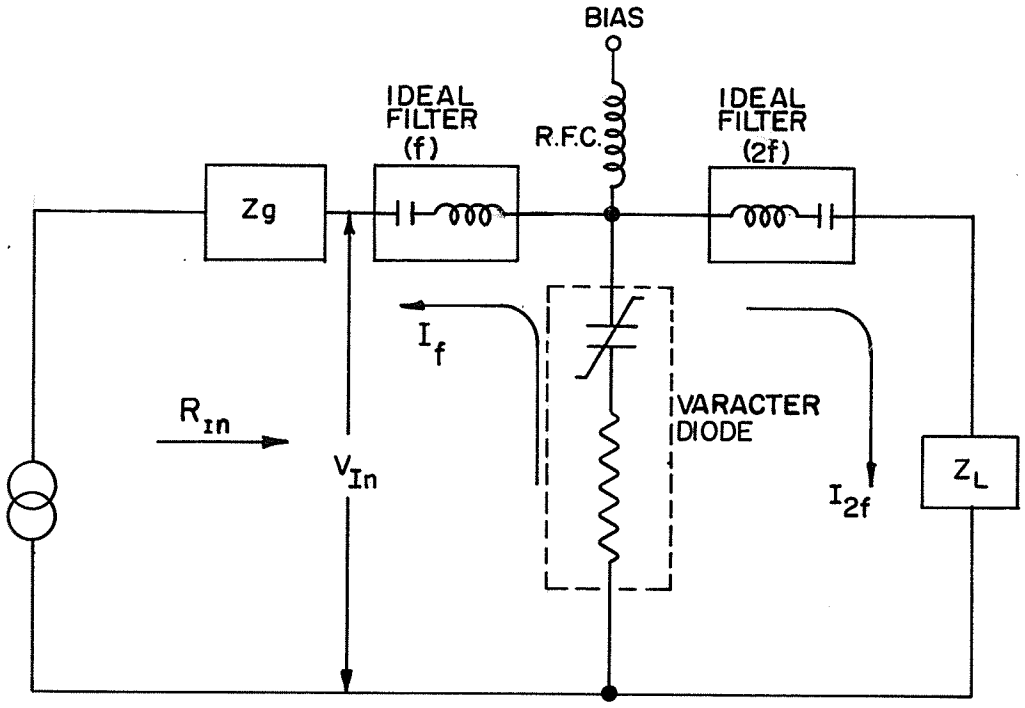

SHUNT TYPE FREQUENCY DOUBLER

FIGURE (3.4)

(a) shunt type frequency doubler*.

(b) series type frequency doubler.

Shunt Type Frequency Doubler:

The circuit shown in Figure (3.4) is used for the shunt type frequency doubler arrangement. The circuit is driven by a sinusoidal voltage source at the fundamental frequency with an internal impedance Z_g. Because of the ideal input filter, which is an open circuit for all frequencies except the fundamental frequency, only the fundamental component of the current can flow in the input loop. A second harmonic current is then generated by the varactor diode and produces useful power in the load Z_L. Furthermore the ideal filter is used in the output loop in order to block the fundamental frequency component of the output current.

Series Type Frequency Doubler:

Depending on the drive, it can have two modes of operation,

1. current pumping mode
2. voltage pumping mode.

A series type current pumped doubler is shown in Figure (3.5a). In this circuit, the varactor is placed in series with two series resonant circuits so that only two currents, one at the fundamental frequency and the other at the second harmonic frequency, are allowed to flow in the diode. The ideal filters are short-circuits at all frequencies except at the specified frequencies.

---

*The Conversion Efficiency for this type of arrangement has been presented in Appendix B.

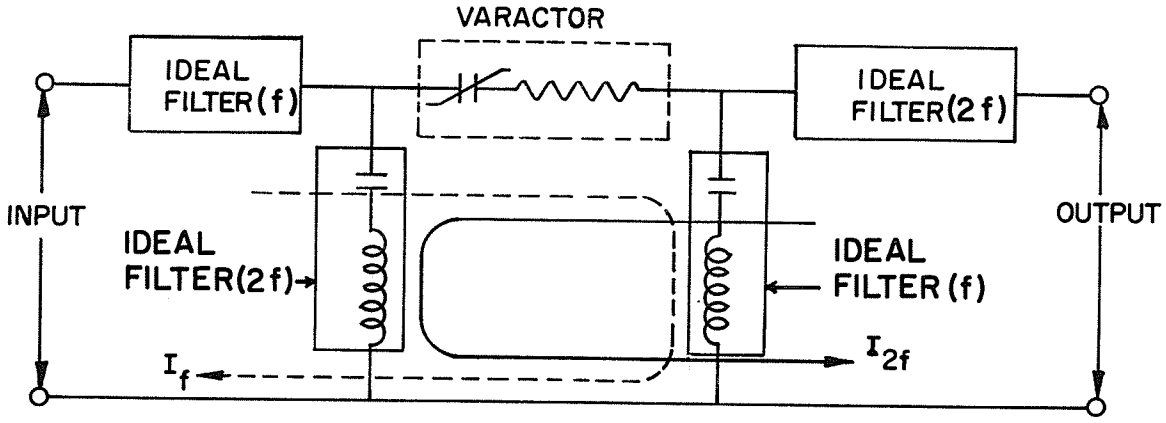

CURRENT PUMPED DOUBLER

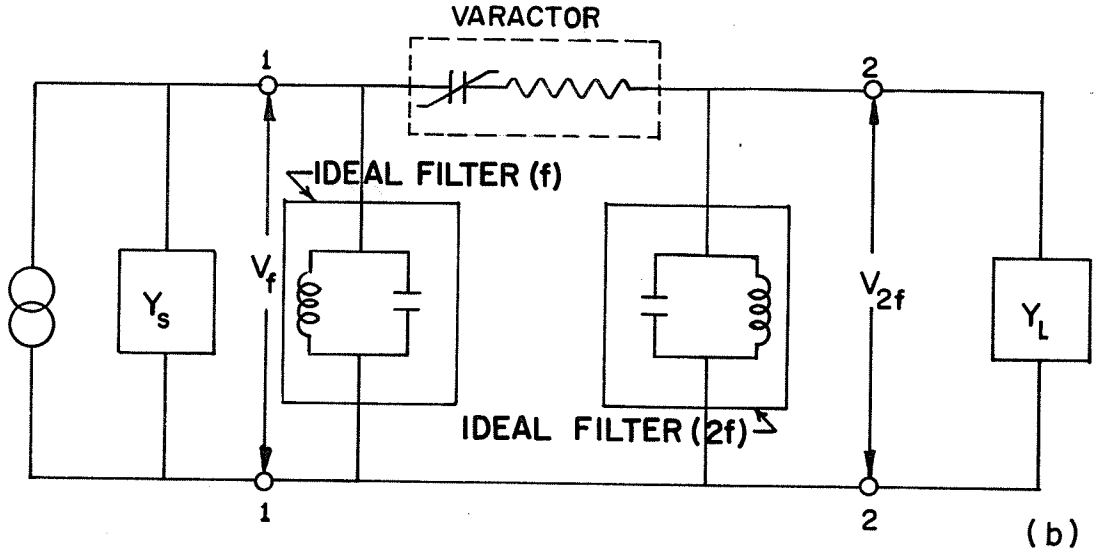

VOLTAGE PUMPED DOUBLER

FIGURE (3.5)

A series type voltage pumped doubler is shown in Figure (3.5b) in which the varactor is in series with two parallel resonant circuits. The ideal filters are short circuits at all frequencies except the one specified. As a result, only the fundamental frequency component of the input voltage can be developed at the input terminals and only power at second harmonic frequency can be delivered to the load admittance Y_L.

CHAPTER IV

HARMONIC GENERATOR DESIGN AND EXPERIMENTAL TECHNIQUES

4.1 CIRCUIT TECHNIQUES:

4.1.1 Crossed Waveguide 4500 MHz - 9000 MHz Doubler.

The harmonic generator investigated, corresponds to the shunt type configuration as already discussed in Chapter III. Here, Figure (4.1) shows the basic elements of this harmonic generator where a crossed waveguide structure is used with the varactor diode located at the intersection of the centre lines of the waveguides. The waveguide in one direction is sized for a fundamental frequency of 4.5 GHz (C band) and in the other direction for second harmonic frequency of 9.0 GHz (X band). A waveguide band-pass filter centred at 9.0 GHz was connected at the output of the generator to exclude the higher harmonics. The power at the harmonic frequency generated by the varactor diode travels down the smaller (or the harmonic) waveguide. The energy at the fundamental frequency, on the other hand, cannot travel into the X-band waveguide since it is beyond cutoff.

Variable tuning plungers terminate the two waveguides as shown in the Figure (4.1) and provide considerable impedance matching for the diode. The optimum position of the two plungers is obtained experimentally. A gradual taper is provided for an efficient coupling of the C and X band waveguides and corresponds to a tolerable impedance match. The dimensions of the tapered section are shown in the Figure (4.1). In

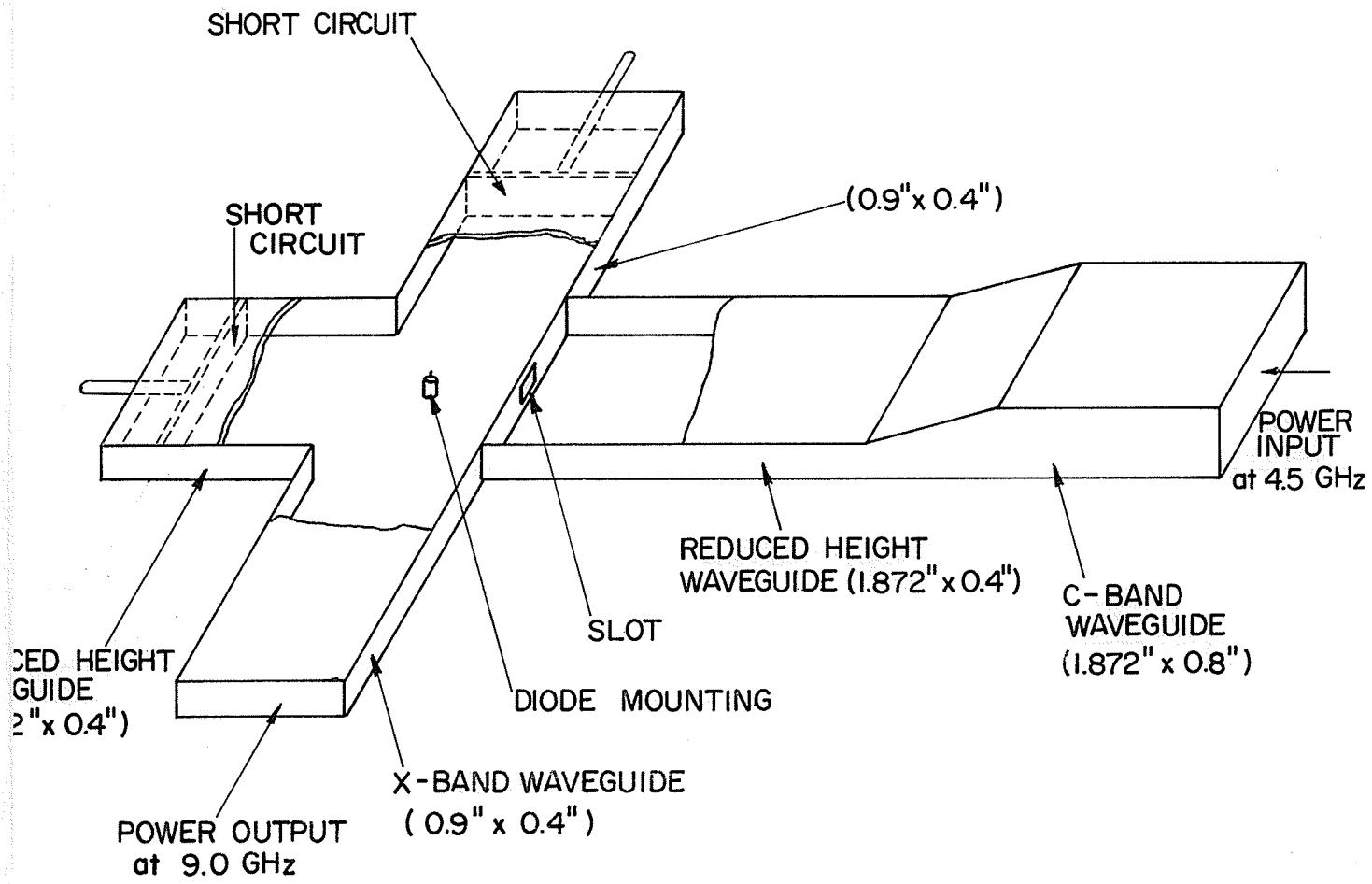

CROSSED GUIDE HARMONIC GENERATOR

fig. 4.1

order to couple the main signal, a slot is provided in the reduced thickness commonwall. A slot controls the amount of energy passing through it. A conducting diaphragm of the form shown in the Figure (4.2) gives the effect of a parallel L-C circuit shunted across the guide at the point at which the diaphragm is placed. For this reason, such a diaphragm is usually called a resonant window. As a first approximation, a resonant window may be considered as a combination of an inductive window and a capacitive window, inserted at some point in the waveguide. The resonant frequency of the window can be changed by changing the dimensions a' and b'. A large number of windows were fabricated and the final dimensions chosen were those corresponding to optimum harmonic power. The optimum dimensions were found to be (0.75" x 0.35"). It has been shown by empirical data [28] that essentially zero susceptance can be obtained at a chosen frequency with a wide variety of slots if the dimensions a' and b' are properly related.

4.1.2 Diode Mounting and Associated Circuitry.

The arrangement for diode mounting is given in Figure (4.3). The mounting was done in such a way that the crystal was accomodated entirely in the smaller waveguide dimensions. The design of the mounting was such that the various mechanical components could be machined separately and assembled (or disassembled) conveniently. As shown different facilities are provided for the ac and dc bias arrangement. There are two teflon filled transmission lines in series with the diode of lengths 0.42" and 0.594" as shown in the figure, and a third air filled transmission line which can be created by moving the adjustable plug for tuning purposes. The characteristic impedances of these lines are 21, 42 and 100 ohms respectively. The normalized input impedances at

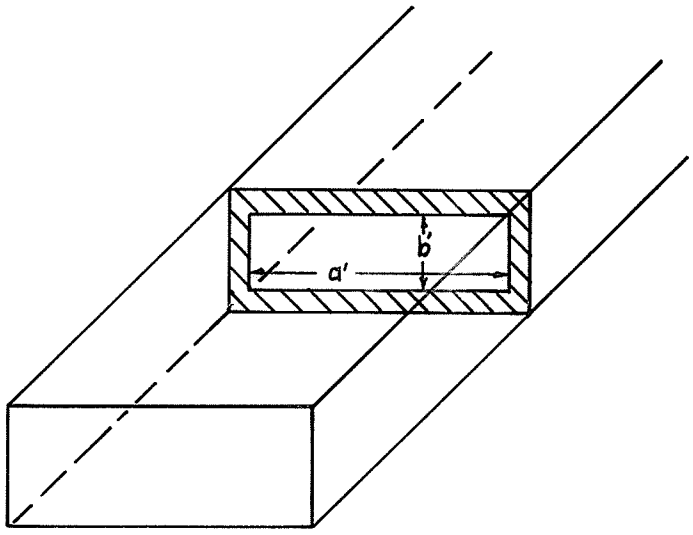

RESONANT WINDOW
IN WAVEGUIDE

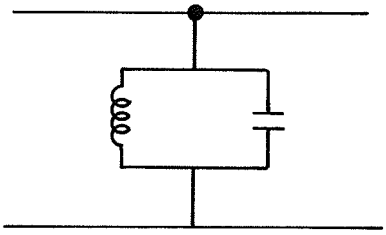

EQUIVALENT CIRCUIT

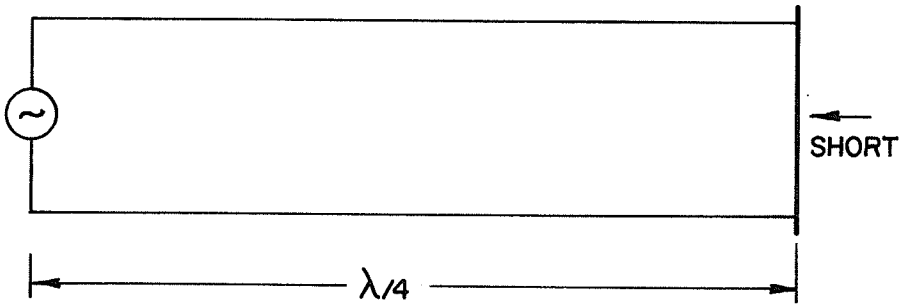

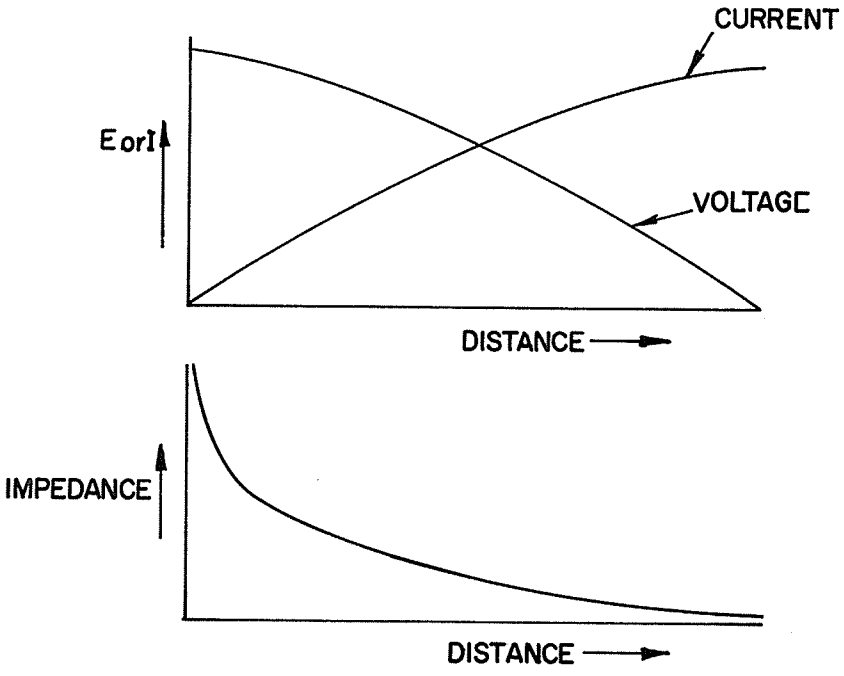

FIGURE (4.2)

at the diode end with respect to 21 ohms line and at the harmonic frequency were computed for various lengths of the air filled line and found to be +j2.25, 0, and -j 2.45 ohms corresponding to the lengths 0.25", 0.0725" and 0", respectively. The actual length of this air filled transmission line was optimized experimentally and found to be approximately the same as the theoretical value.

A co-axial to waveguide coupler is used for feeding the oscillator power and a waveguide to co-axial coupler for extracting the power from the harmonic generator. At the waveguide junction where the diode is mounted, there are four possible paths in which the energy can travel. However, the objective is to ensure that the maximum harmonic energy travels towards the output waveguide. The fundamental power cannot propagate in the X-band harmonic guide since the dimensions of this waveguide are beyond cutoff. The harmonic energy cannot travel back towards the fundamental guide due to the resonant window which becomes antiresonant at the harmonic frequency. Harmonic power is made to travel only towards the output waveguide by terminating the other two arms by movable short circuits. By adjusting the distance of the plungers from the diode, an infinite impedance to waves at the harmonic frequency is created in that direction. This is because when a line, which is an odd multiple of quarter wavelengths, is terminated in a short circuit, then it would represent a very high impedance at the input end. This can be seen by the voltage and current distribution on a $\lambda/4$ short circuited line as shown in Figure (4.2). This can also be interpreted from a power point of view since the short circuiting plungers are adjusted to match the incident power to the diode.

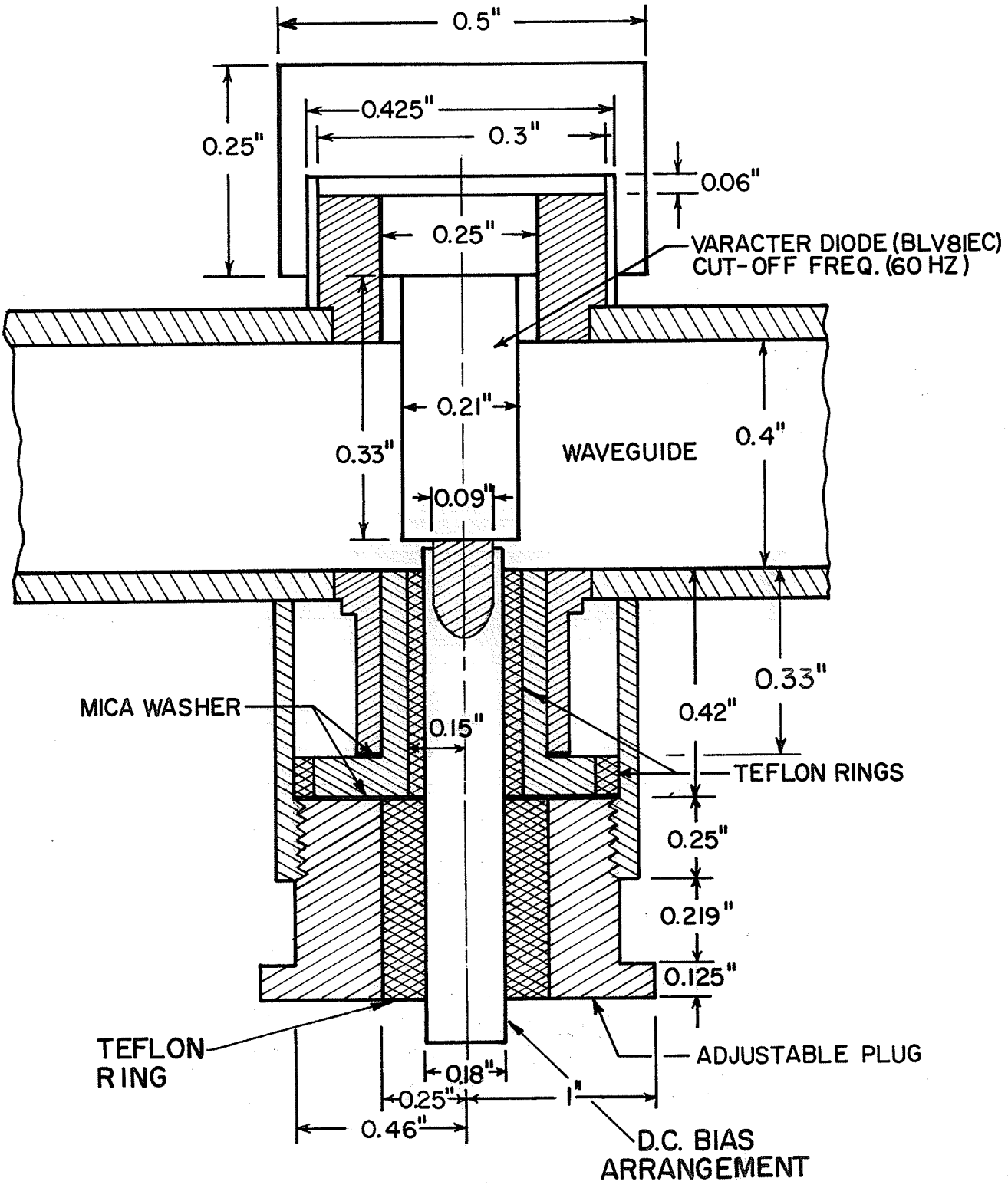

DIODE MOUNTING

Fig. 4.3

4.2 EXPERIMENTAL WORK:

4.2.1 V-I Characteristics of the Varactor Diode.

Since it is necessary to know the V-I characteristics of the varactor diode, an experimental set up for this purpose is shown in Figure (4.4). Different readings for voltage and current are taken for forward and reverse bias. A plot of V-I characteristics is shown in the Figure (4.4).

4.2.2 Voltage-Capacitance Characteristics of a Varactor Diode.

In order to measure the voltage-capacitance characteristic, the varactor diode should be mounted correctly, and well-matched to the associated circuits. Much work has been done in this direction to optimize the various diode mounts for various varactor diodes. In our experimental work the varactor diode is placed in an X-band crystal mount.* The experimental set up is shown in the block diagram of Figure (4.5).

To begin with, an open circuit diode is placed in the mount while V.S.W.R. and position of voltage minimum are recorded. The open circuit diode is then replaced by a short circuited diode and again the V.S.W.R. and the distance between the reference plane and the position of voltage minimum are recorded and the data is plotted on a Smith Chart. Now the actual diode is placed in the mount and the V.S.W.R. and the position of a minimum are recorded. The reactance of the short circuit point is read on the Smith Chart and subtracted algebraically from the reactance measured by the actual diode to get the junction reactance. Excellent discussion on the topic "When a diode shunts a transmission line" is available in the literature [29]. This author discusses the shunt-mounted diode in the form of an equivalent circuit as shown in Figure (4.5a). There, Z_a is the impedance shunting the guide and therefore

---

*The mount used is HP 485 B.

VOLTAGE	CURRENT
0.125 V	0 μA
0.2	6
0.3	25
0.4	55
0.475	80

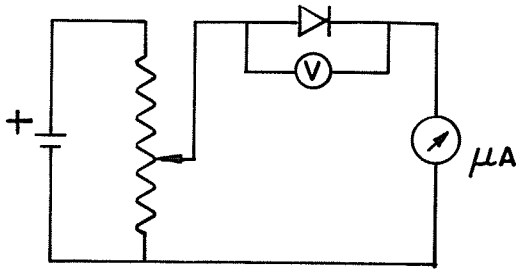

CUT OFF FREQ. = 60 GHz

V_B = 6 VOLTS

C_j = 0.179 Pf

R_s = 2.5 Ω

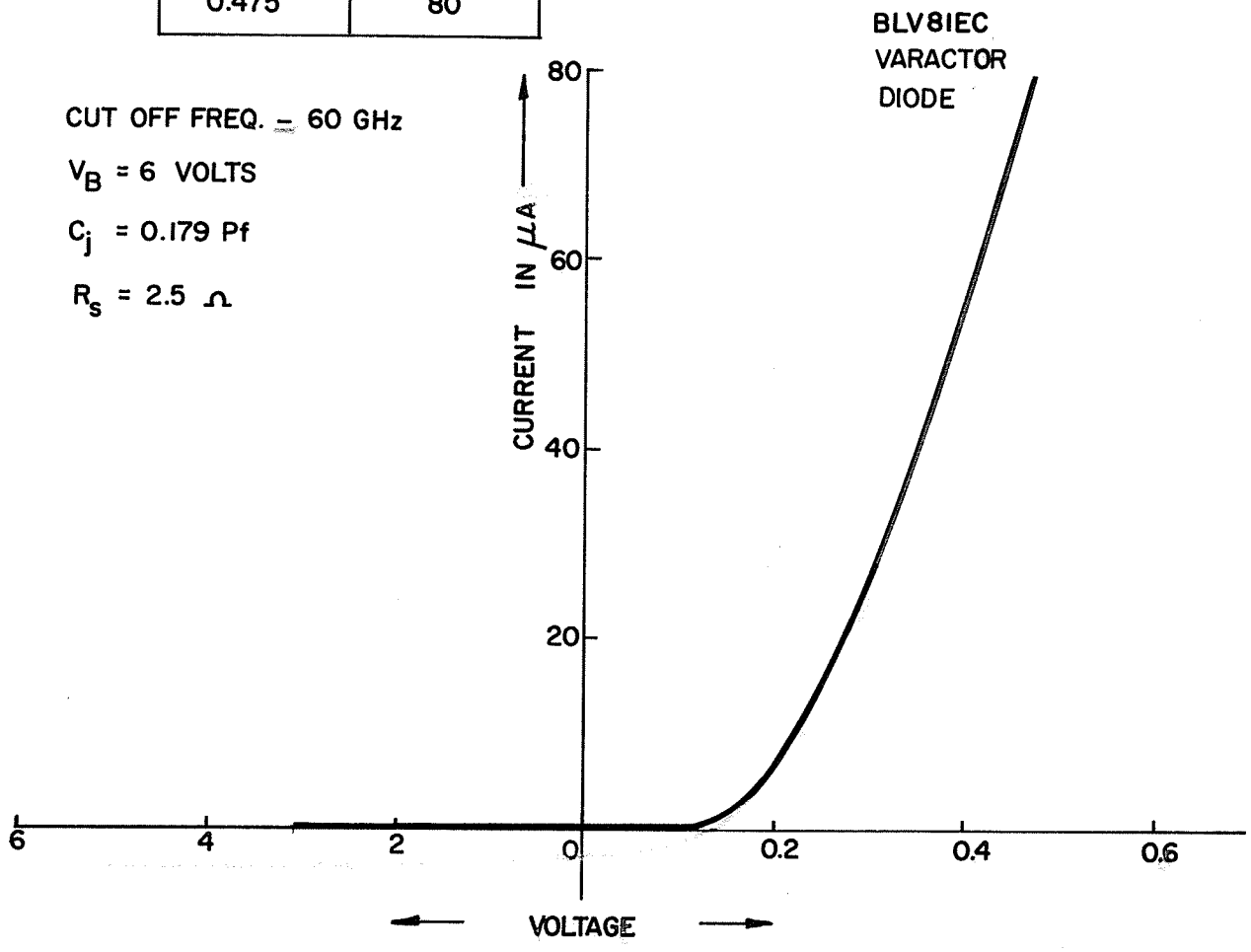

V-I CHARACTERISTICS

FIGURE 4.4

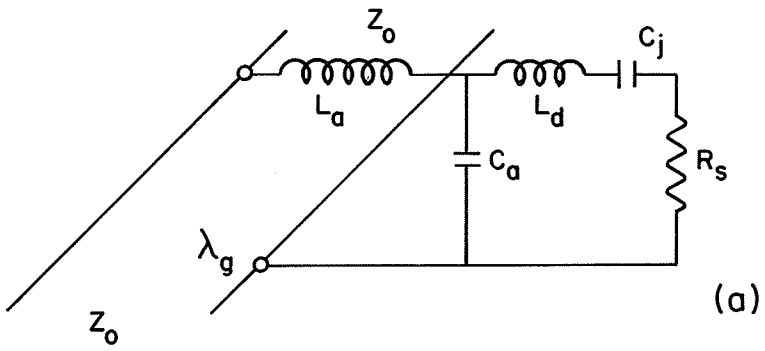

EQUIVALENT CIRCUIT OF A DIODE MOUNTED IN A WAVEGUIDE

SET-UP FOR MEASUREMENT OF VARACTER CAPACITANCE

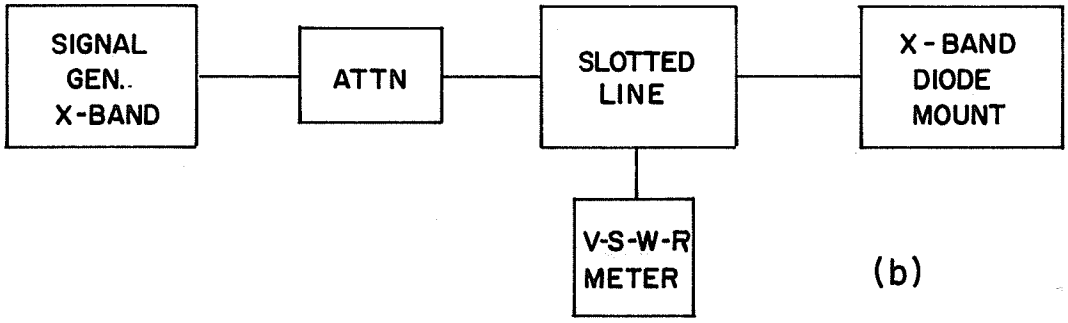

NEGATIVE BIAS VOLTAGE	CAPACITANCE
0.1 V	15 PF
0.5	8
1.0	6
1.5	2.2
2	3.5
2.6	2
3	1
5	1

FIGURE 4.5

$$L_a = \frac{X_a}{\omega} \qquad (4.2.1)$$

C_d is the parallel plate capacitance of the mount within the diode package and is given by

$$C_d = \frac{\pi d^2}{4h}\ \varepsilon_o \qquad (4.2.2)$$

where d and h are the diode package diameter and mount parallel plate spacing, respectively, and ε_o is the permittivity of air. L_d and C_A are the package inductance and capacitance. C_j and R_s are the junction capacitance and the series resistance.

Whereas every effort has been taken to take the inductance L_a into account, its effect is not completely understood in the assumed model and could therefore lead to serious error. Bias voltage vs capacitance is plotted in Figure (4.6). The capacitance assumes a minimum value at breakdown voltage. The minimum capacitance measured is about 1 pf whereas the tabulated value of the capacitance by the manufacturer is less than 0.2 pf. The error could be due to the unmatched diode mount.

4.2.3 Measurement of Filter Insertion Loss.

Since it is necessary to know the insertion loss presented by the band-pass filter, an experimental set-up for this purpose is shown in

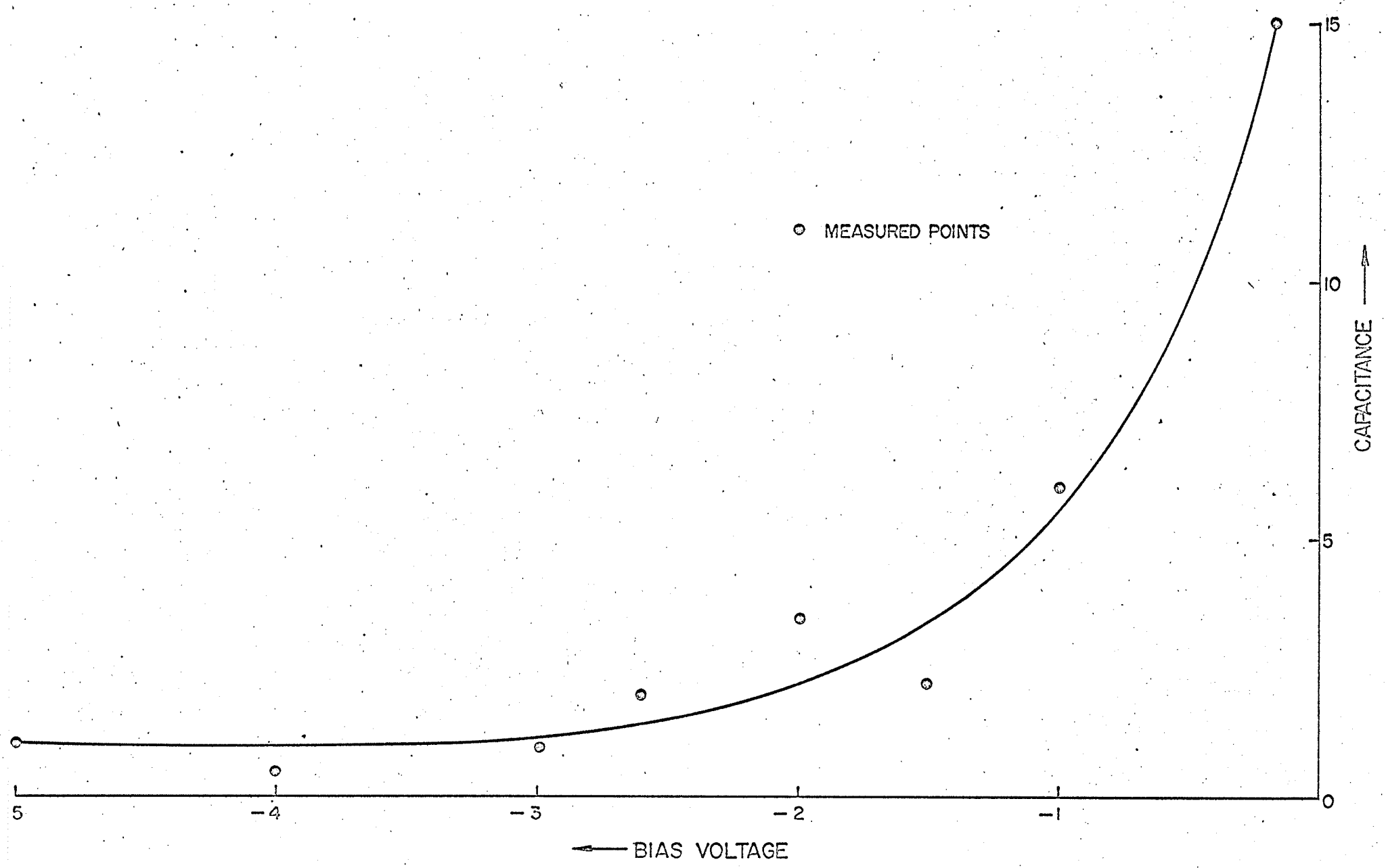

FIGURE 4.6

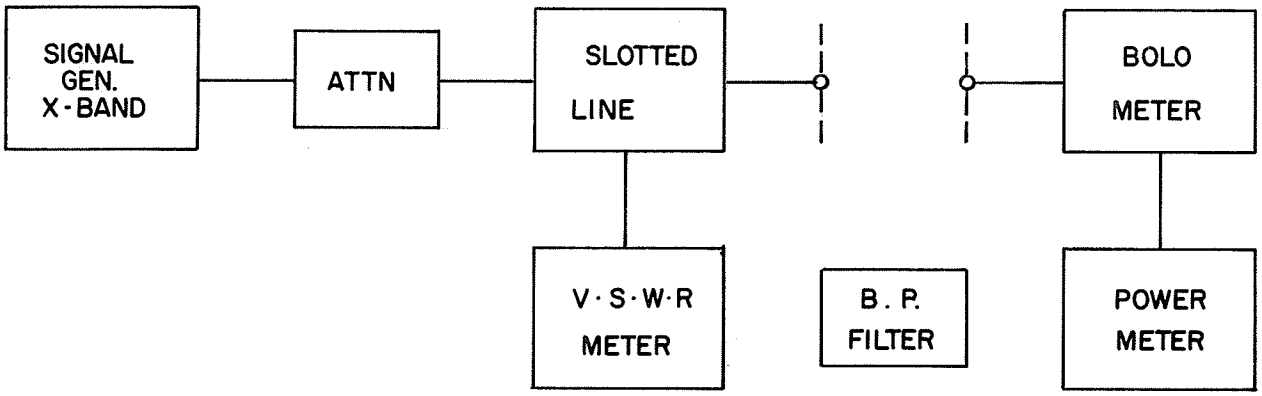

SET-UP FOR MEASUREMENT OF FILTER CHARACTERISTICS

FREQUENCY GHz	INSERTION LOSS 10 log P_1/P_2
8.825	28 db
8.85	22
8.90	13.5
8.95	4.25
9.00	2.5
9.025	2.7
9.05	8
9.10	16
9.15	27

P_1 IS POWER READ ON METER WITHOUT THE FILTER CONNECTED

P_2 IS POWER READ WITH THE FILTER CONNECTED

FIGURE 4.7

Figure (4,7). The complete design of this filter is given in Appendix C. The usual method of "power-ratio measurements" is used to measure the insertion loss of the filter.

To begin with, load power P_2 is measured on the power meter with the band-pass filter connected in the system, after which the band-pass filter is removed and load power P_1 is again measured with nothing else changed. The ratio of P_1 to P_2 converted to db gives the insertion loss in db's. The above procedure is repeated for different frequency settings of the signal generator to get a plot of frequency vs insertion loss as shown in the Figure (4.8). It can be seen from these characteristic that the insertion loss presented by this filter is about 2.5 db.

V.S.W.R. for the band-pass filter is 2.5 hence Γ, the reflection coefficient, is 0.425. The mismatch loss is given by:

$$\alpha_m = \frac{1}{1 - |\Gamma|^2}$$

hence $\alpha_m(db) = 10 \log \frac{1}{1 - |\Gamma|^2} = \underline{0.85 \text{ db}}$

now

Insertion loss = attenuation loss + mismatch loss

i.e. $(\alpha_i) = (\alpha_a) + (\alpha_m)$

hence

$$\alpha_a = \alpha_i - \alpha_m = 2.5 - 0.85 = \underline{1.65 \text{ db}}.$$

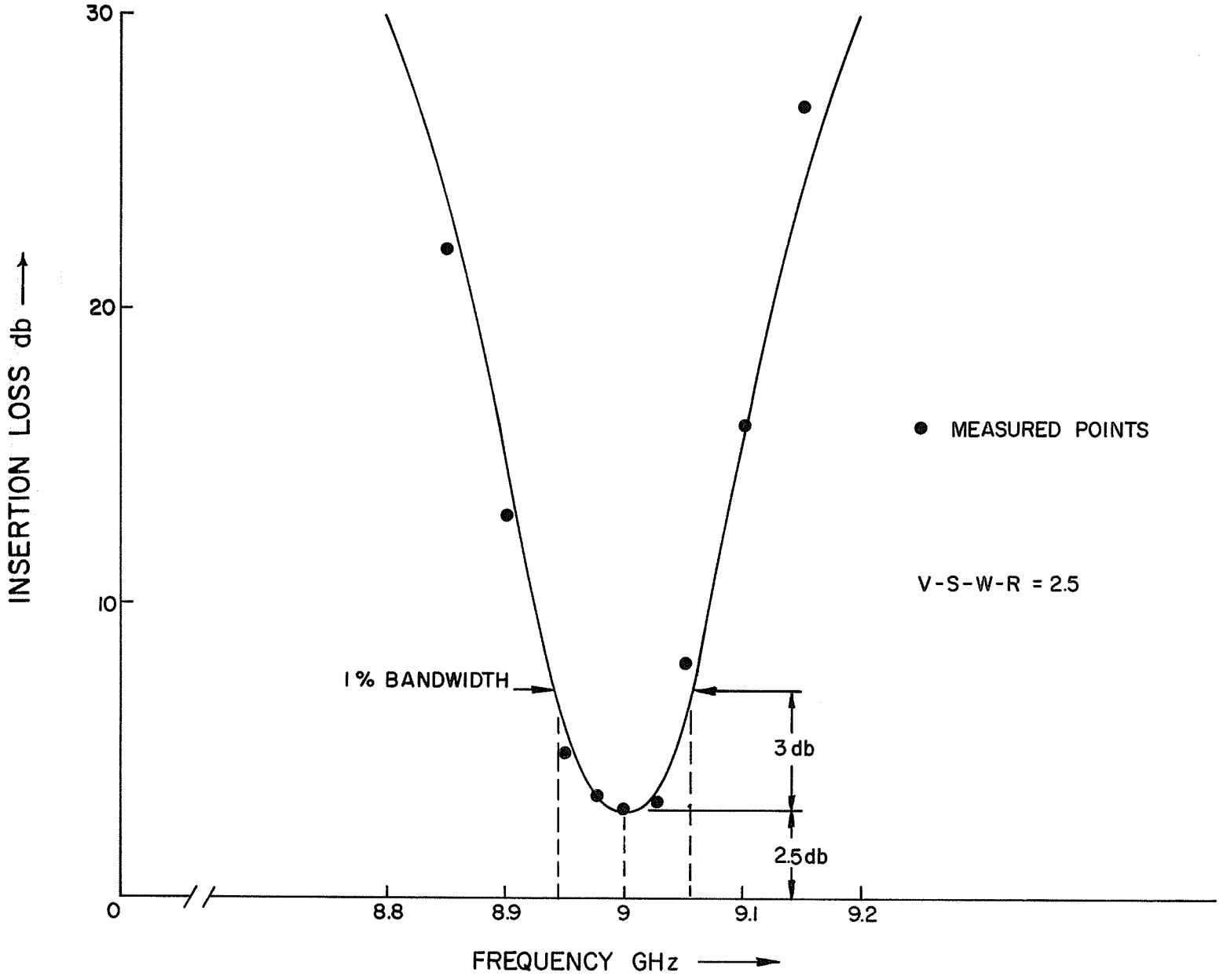
30
20
10
0
INSERTION LOSS db
8.8
8.9
9
9.1
9.2
FREQUENCY GHz
MEASURED POINTS
V-S-W-R = 2.5
1% BANDWIDTH
3 db
2.5db

FIGURE 4.8

The specifications of the band-pass filter used in the harmonic generator are

Upper pass-band frequency = 9.05 GHz

Lower pass-band frequency = 8.95 GHz

Center frequency = 9 GHz

Bandwidth = 1%

V.S.W.R. = 2.5

Insertion loss = 2.5 db.

4.3 EXPERIMENTAL PROCEDURE:

4.3.1 Detection of Output Power From the Harmonic Generator.

The experimental setup used to detect the power output in the harmonic generator is shown in the block diagram of Figure (4.9). The output of the harmonic generator is connected through a crystal to a very sensitive crystal bolometer amplifier. The signal source is modulated by a 1 KHz signal and the signal generator frequency is set at 4.5 GHz. The power detected is maximized by the simple adjustments of the short-circuit plunger, the coupling slots, as shown in the (Figure 4.1).

4.3.2 Measurement of Harmonic Power.

The harmonic power was measured in two different ways:

(1) direct method,

(2) comparison method.

The setup for the direct method is shown in the block diagram of Figure (4.9). A co-axial tuner is used for transferring the maximum power.

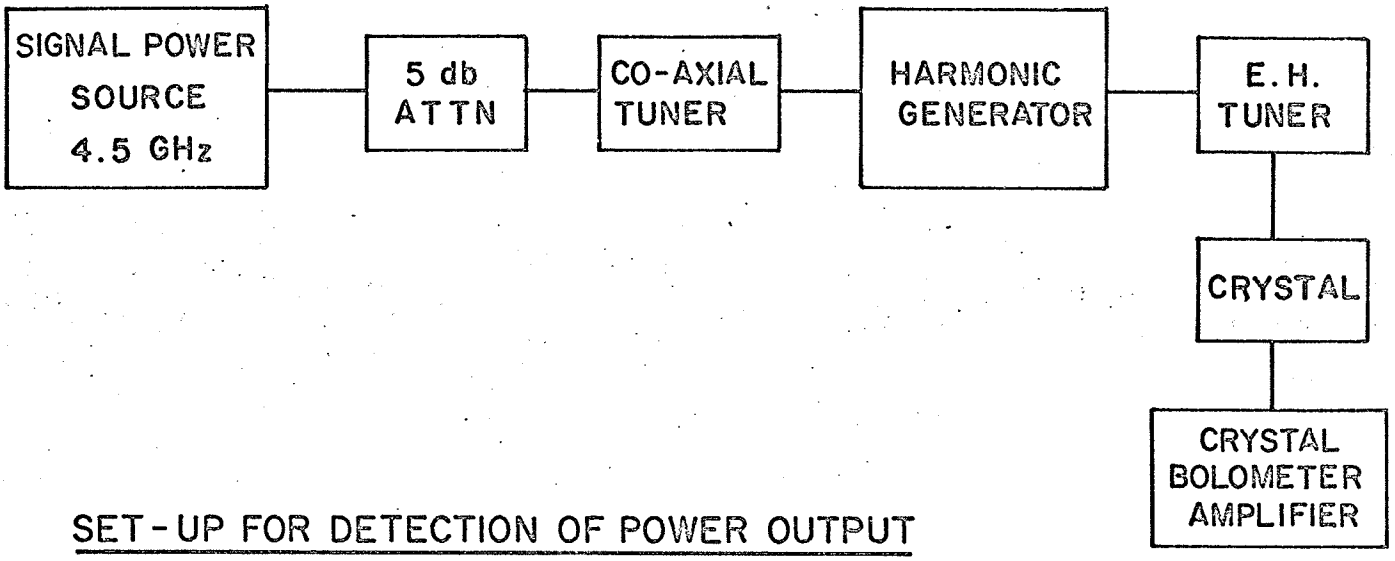

SET-UP FOR DETECTION OF POWER OUTPUT

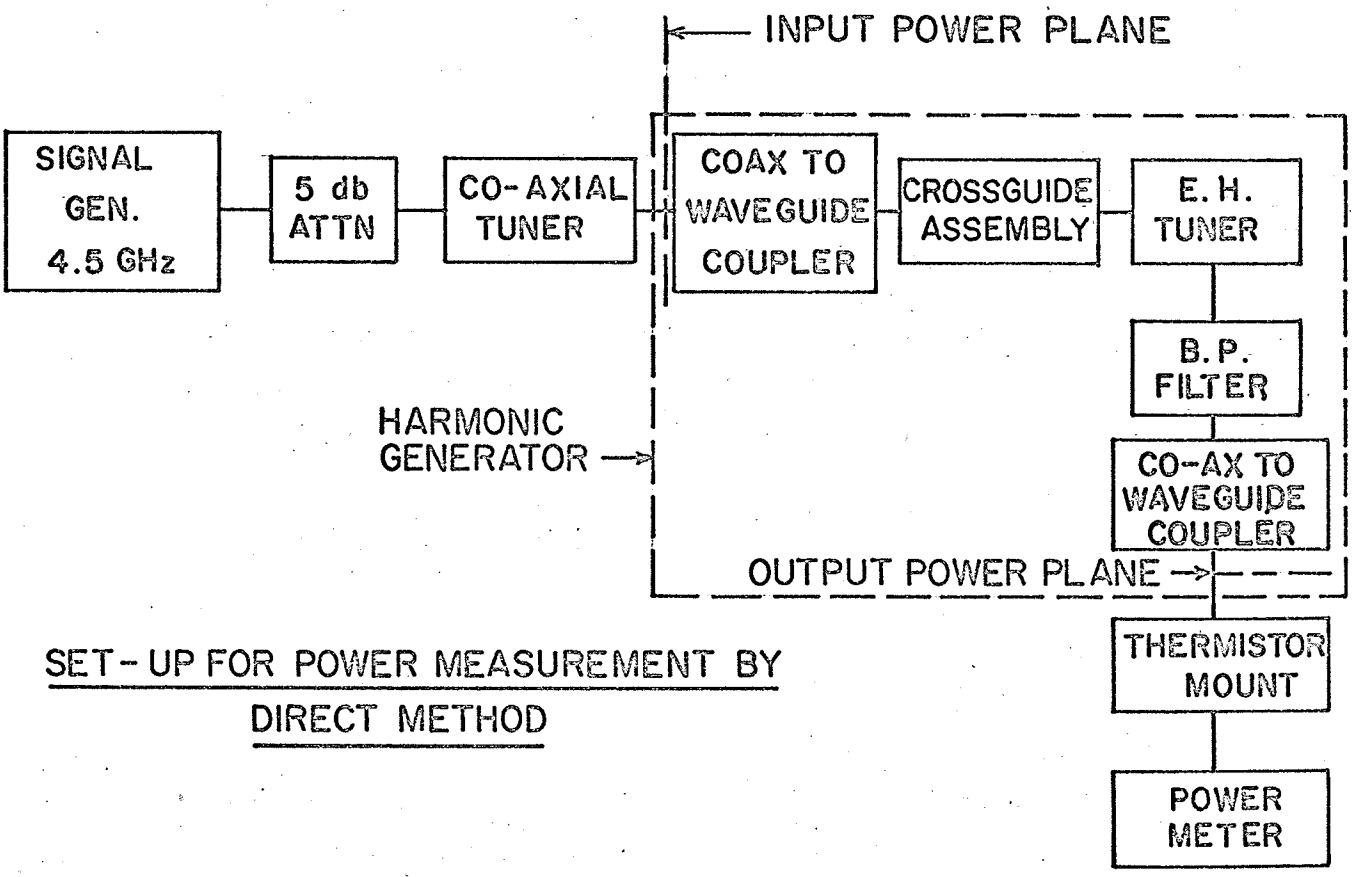

SET-UP FOR POWER MEASUREMENT BY DIRECT METHOD

Fig. 4.9

from the signal generator to the fundamental guide of the harmonic generator by matching the output impedance of the signal generator to the fundamental waveguide impedance. Similarly an E-H tuner is used on the output side of the harmonic generator to deliver maximum power to the band-pass filter. The output of the band-pass filter is connected to a power meter through a thermistor mount. The signal generator frequency is set at 4.5 GHz and maximum output power is obtained by making the adjustments already described in section (4.3.1). The harmonic generator is disconnected at the output of the stub tuner and connected directly to the power meter. The stub tuner is retuned to get the maximum power output from the signal generator. The difference in db between the two readings gives the conversion loss of the harmonic generator in db.* The distance of the short circuits from the varactor diode and the dimensions of the coupling slot used to get the maximum power output are also noted. Since the power meter scale is limited to 10 milliwatts, the output power of the harmonic generator is adjusted so that the maximum value does not exceed the full scale of the meter reading. Different readings are taken with different input power levels, and a plot of corresponding conversion loss is given in Figure (4.12).

Figure (4.10) shows a photograph of the experiment described above. The wavemeter connected between the thermistor mount and the band-pass filter is removed for power measurements, and is included only for frequency measurements.

The set up for the second method (comparison method) is the same as shown in the block diagram of Figure (4.9), except that the thermistor mount and the power meter are now replaced by a crystal and

---

*The contributions from the harmonics other than the 9.0 GHz signal were found to be -16db for 13.45 GHz, -19db for 16.8 GHz and -21db for 15.1 GHz signals (with respect to 9.0 GHz signal)using a spectrum analyzer.

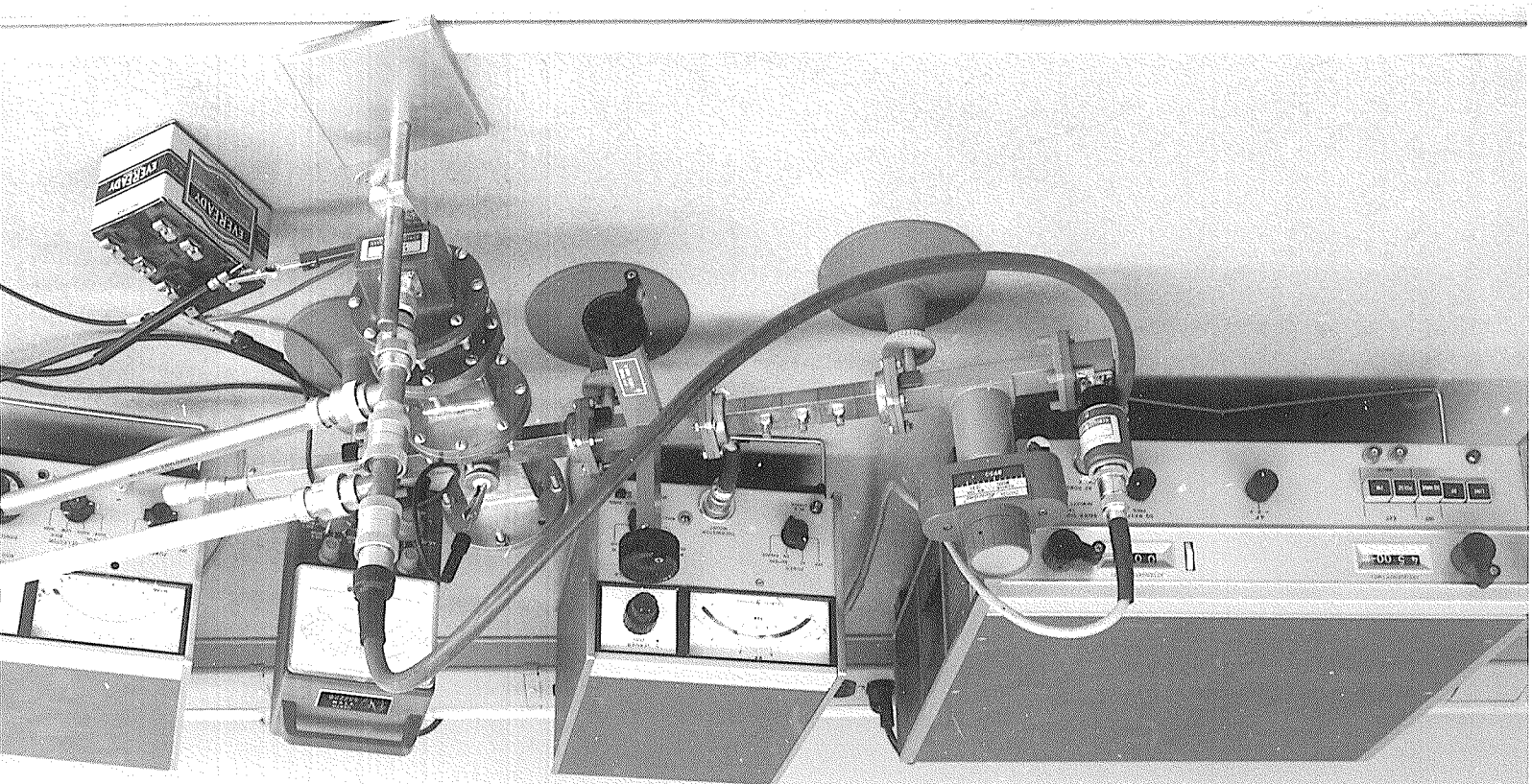

a V.S.W.R. meter. The input power to the harmonic generator is controlled by an attenuator attached to the signal generator. The signal generator frequency is set at 4.5 GHz and is modulated by a 1 KHz signal. The maximum reading obtained on the meter, by making the adjustments already described, is noted in db and the attenuator reading on the signal generator is also noted. The output of the signal generator is then detected and connected directly to the V.S.W.R. amplifier. The attenuator on the signal generator is varied to get the same readong on the V.S.W.R. amplifier as before. The difference of the two attenuator readings gives the conversion loss in db. The attenuator readings are then adjusted by corrections obtained from a calibration curve made with the power meter.

The results for the conversion loss based on the two methods are given in the table and are based on the calibration given in Table I.

4.3.3 Measurement of Frequency.

The set up for the frequency measurement is the same as shown in the block diagram of Figure (4.9) except that a wavemeter covering the X-band range is now connected between the filter and the thermistor mount as shown in the Photograph of Figure (4.10). The wavemeter is adjusted until the output frequency from the harmonic generator becomes resonant with the cavity of the wavemeter; at the point of resonance a dip in the power meter reading will be noticed. The frequency is then read directly from the calibrated scale of the wavemeter.

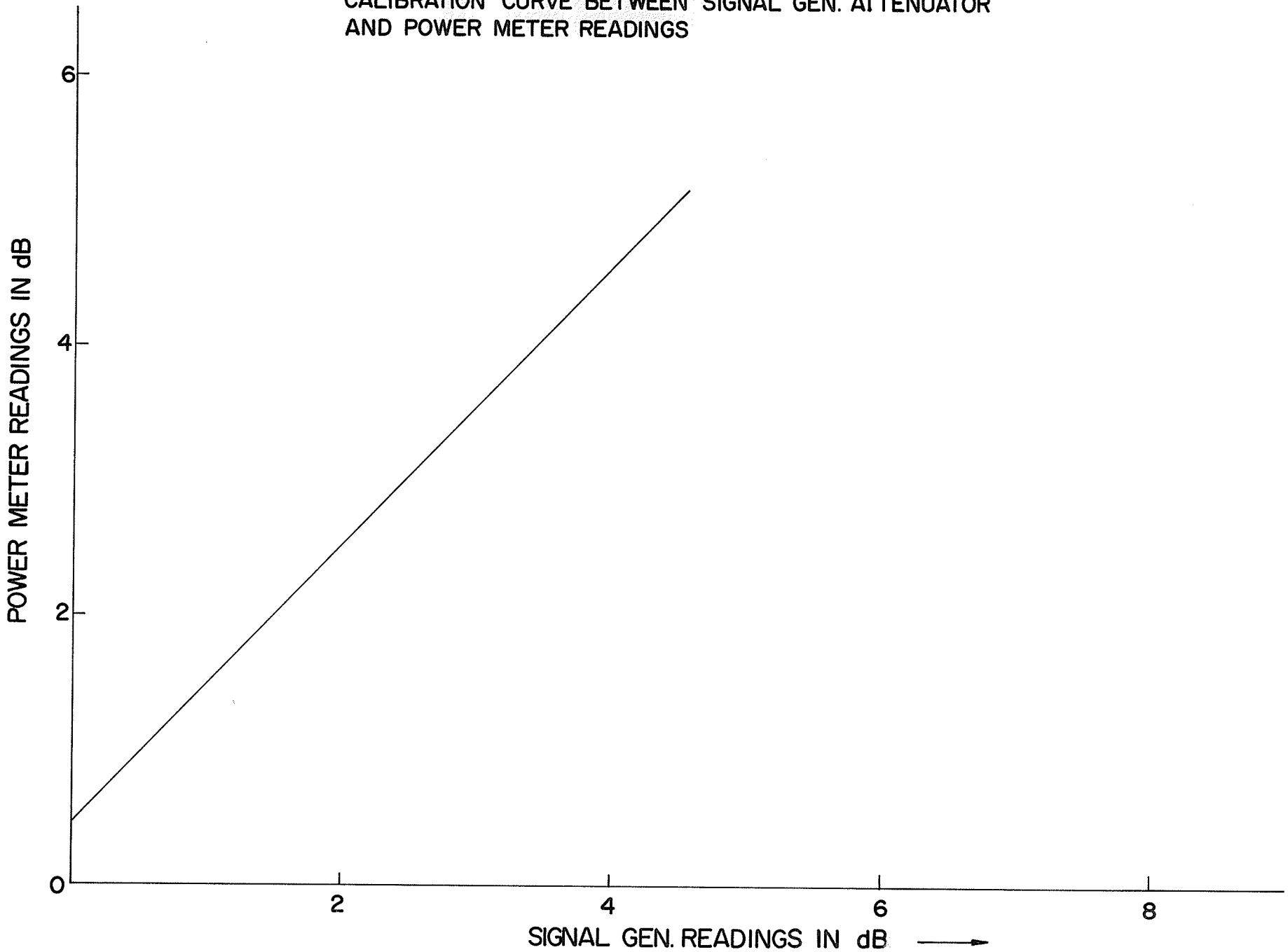
CALIBRATION CURVE BETWEEN SIGNAL GEN. ATTENUATOR
AND POWER METER READINGS
POWER METER READINGS IN dB
0
2
4
6
2
4
6
8
SIGNAL GEN. READINGS IN dB

FIG. 4.11

RESULTS:

DIRECT METHOD*

Input Power milliwatts	Conv. Loss in db	Theoretical Conv. loss in db
2.0	5.0	1.6
2.5	4.0	1.6
3.7	3.8	1.6
5.2	4.1	1.6
7.5	4.0	1.6

COMPARISON METHOD

Input Power milliwatts	Conv. Loss in db	Conv. Loss After applying correction	Theoretical
3.0	3.45	4.0	1.6
5.0	3.45	4.0	1.6
7.0	4.4	3.9	1.6
10.0	4.5	3.95	1.6

TABLE I

Output frequency measured by the cavity wavemeter = 8.99 GHz

Bias voltage used = 1.5 volts

Dimensions of the coupling slot which gives maximum output = 0.75" x 0.35"

Distance of short circuit in the X-band waveguide from the diode = 1.58 inches.

Distance of short circuit in the reduced height waveguide from the diode = 0.75 inches.

---

* The direct method was primarily for the sake of tuning the harmonic generator.

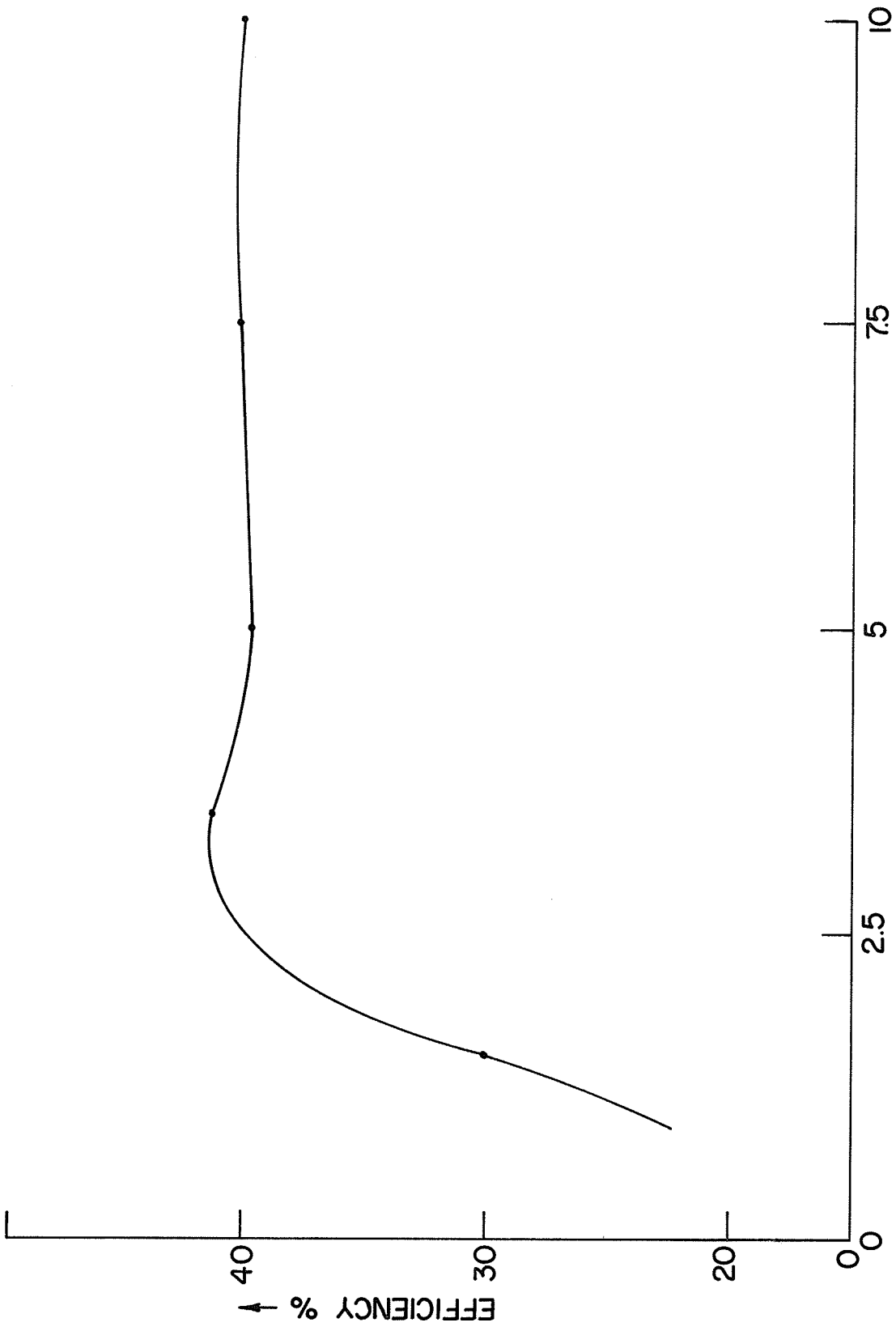

fig. 4.12

CHAPTER 5

DISCUSSION AND CONCLUSIONS

5.1 GENERAL DISCUSSION:

Frequency multiplication can be achieved in a very efficient way through the use of a non-linear reactance. Since, the non-linear reactance is a low noise device, the resulting efficiency obtainable provides the possibility of using it as a multiplier of considerably high order without introducing additional or excess noise from the active elements.

Complete conversion of fundamental power to power at any harmonic is not impossible provided that we have an ideal non-linear reactance element. The difficulty in obtaining efficient multipliers in the microwave range is due to the excessive loss presented by the diode, the associated circuitry and the unwanted harmonics. A significant increase in efficiency is obtained when the undesired harmonics are prevented from being generated and their power is returned to useful output at the desired harmonic frequency.

The efficiency of the harmonic generator is a definite function of Q of the diode. For higher frequency operation, the loss of the diode will be much greater than other circuit losses. A diode with high Q is therefore essential. The input power to the varactor diode is limited by reverse breakdown voltage of the diode. When the diode is biased at high negative voltage, the input voltage can be increased proportionally without the diode conducting in the forward region. It may

also be noted that certain harmonics may not be obtained with particular characteristics and circuit configurations. For example, a capacitance of the form $C = \frac{k}{(V + \phi)^{\frac{1}{2}}}$ will generate no harmonics higher than the second in the shunt type configuration of doubler since all of the higher order Taylor coefficients are zero. So for generating high order harmonics we should use the series type configuration. On the other hand, the shunt type of doubler can handle more power than a series type. The maximum power which can be handled may be limited by one of two factors. These are: the voltage across the non-linear capacitance which cannot exceed the total bias voltage or breakdown voltage; secondly the I^2R losses in the varactor must remain below a reasonable value. In general, the power which can be handled by the frequency multiplier is greater for lower impedance circuits. The shunt type configuration has the advantage in this respect and has been capable of handling several hundred milliwatts without reduced efficiency.

The graph in Figure 4.12 represents an experimental curve of input power vs efficiency for the frequency doubler. The graph shows that at high input power levels, the response is quite flat. The response of the doublers very was not measured at/high input power levels for lack of suitable equipment. It is expected that as input power becomes larger, the measured efficiency should tend to drop.

It was believed that the reason for deviation between theoretical and experimental results was due to the losses in the waveguide, and associated components e.g. loss in the band-pass filter and losses in the impedance matching components. Another reason for deviation between theoretical and experimental results could be due to the fundamental power not being fully utilized by the diode. The fundamental energy

can leak towards the dc supply arrangement. The fundamental energy could be blocked from leaking by providing co-axial chokes as used by Steele [30]. The general theory for co-axial chokes is given by Ragan [31].

5.2 CONCLUSIONS:

The construction of a 4.5 to 9.0 GHz varactor frequency doubler with a conversion efficiency of approximately 38% has been achieved since approximately 2% of the measured power is attributed to the third harmonic (13.5 GHz). It is believed that there are yet several ways of obtaining improvement in the circuit efficiency. The applications of presently well known techniques for making precision electroformed waveguides to the construction of varactor diode mounts of reduced height waveguide, should provide a much better impedance match to the diode and should reduce the overall conversion loss.

The use of varactor arrays in frequency multipliers to provide increased output power have been reported recently [32]. Also a series array has been used to raise the impedance level such that the circuit losses become a less significant fraction of the input and output load impedances thus providing more efficient operation.

Certain transistors have also been recently used for the dual purpose of amplification and frequency multiplication [33] where the collector to base capacitance acts as a varactor. Although transistor multipliers are simpler to operate at perhaps less cost, their output is smaller than that obtained by using a varactor multiplier.

For moderate power requirements, it may be desirable to use transistor amplifier /multipliers up to about 1 GHz and varactor multipliers

for higher frequencies. In the case of high output power and broad dynamic range requirements, the step recovery diode is ideal [34]. For moderate power and dynamic range requirements the abrupt junction varactor is quite suitable at present.

5.3 SUGGESTION FOR FUTURE RESEARCH:

The recently introduced "step-recovery" diode [34] appears to be an ideal device for applications requiring high power, broad dynamic range and reasonably high efficiency. The term "step recovery" refers to the phenomenon of sudden collapse in reverse current as charged carriers, which cross the junction during the positive part of the cycle, return to their point of origin. It is this sudden collapse of current which produces a waveform that is rich in harmonics, thus enhancing multiplier action. These diodes can handle about twice as much power as abrubt junction varactors. Typical power handling probability is in the 2-watt range at X-band (10 GHz). It is therefore suggested that use of this diode be investigated in future multiplier development.

APPENDIX A

A.1 VOLTAGE DEPENDENT BARRIER CAPACITANCE

The space charge diagram of an abrupt junction is shown in Figure (2.2a). Here q is the electronic charge while N_d and N_a are the doping concentrations for the donors and the acceptors respectively. The space charge in the n-region is $q N_d$ while $-q N_a$ is the charge in the p-region.

Applying Poisson equation to this configuration we have;

$$\frac{d^2\phi}{dx^2} = -\frac{\rho}{\varepsilon_o} \qquad (A.1)$$

where ϕ is the electric potential, ρ is the charge density, and to a good approximation, is given by $q(N_d - N_a)$ for $-x_a < x < x_b$. Furthermore:

$$\ell = 0, \; -\infty < x < -x_a$$

$$N_d = 0, \; -x_a < x < 0$$

$$N_a = 0, \; 0 < x < x_b$$

The boundary conditions applicable in this case are:

$$x = -x_a \quad \text{when } \phi = \phi_a \quad \text{and} \quad \frac{\partial\phi}{\partial x} = 0$$

$$x = x_d \quad \text{when } \phi = \phi_b \quad \text{and} \quad \frac{\partial\phi}{\partial x} = 0 \qquad (A.2)$$

ϕ and $\frac{\partial\phi}{\partial x}$ both must be continuous at $x = 0$.

Solving equation (A.1) and applying the boundary conditions, the junction capacitance $C(V)$ per unit area is given by [35].

$$C(V) = \frac{\varepsilon_o}{x_a + x_b} = \left[\frac{\varepsilon_o \, q \, N}{2(\phi_b - \phi_a + V)} \right]^{\frac{1}{2}} \qquad (A.3)$$

where $N = \dfrac{N_d N_a}{N_a + N_d}$

and V represents the magnitude of external bias applied in the reverse direction. $\phi_b - \phi_a$ is the contact potential and denoting it by ϕ we have

$$C(V) = \frac{K}{[\phi + V]^{\frac{1}{2}}} \qquad (A.4)$$

where K is a constant given by

$$K = \frac{\varepsilon_o \, q \, N_a \, N_d}{2(N_a + N_d)}$$

A.2 VARACTOR DIODE AS A CIRCUIT ELEMENT:

In general, the non-linear depletion layer capacitance is given by:

$$C(V) = K(\phi + V)^{-n} \qquad (A.5)$$

where n is an exponent depending upon the impurity doping on both sides of the junction. For abrupt junctions n equals $\frac{1}{2}$ and for graded junctions n equals $\frac{1}{3}$. This capacitance has a minimum value at the breakdown voltage V_B. i.e.:

$$C_{min} = K(\phi + V_B)^{-n} \qquad (A.6)$$

and hence

$$K = C_{min} \, (\phi + V_B)^n \qquad (A.7)$$

Substituting in (A.5) we obtain:

$$C(V) = C_{min} (\phi + V_B)^n (\phi + V)^{-n} \qquad (A.8)$$

C(V) can also represented by a charge or junction current with the voltage as the independent variable.

$$C(V) = \frac{dQ}{dV} \qquad (A.9)$$

or

$$Q = \int C(V)\, dV$$

$$Q = \frac{C_{min} (\phi + V_B)^n (\phi + V)^{1-n}}{1 - n} \qquad (A.10)$$

The current in the capacitor is given by taking the derivative of Q with respect to time

$$I = \frac{dQ}{dt} = C_{min} (\phi + V_B)^n \phi^{-n} \left[1 + \frac{V}{\phi}\right]^{-n} \frac{dV}{dt} \qquad (A.11)$$

When an a.c. signal is superimposed on a fixed d.c. bias voltage V_e i.e.

$$V = V_e + V_{a.c.} = V_e + v \qquad (A.12)$$

hence

$$I = C_{min} (\phi + V_B)^n (\phi + V_e)^{-n} \left[1 + \frac{v}{\phi + V_e}\right]^{-n} \frac{dV}{dt} \qquad (A.13)$$

Expanding the above equation into a binomial series we have:

$$I = C_{min} (\phi + V_B)^{n} (\phi + V_e)^{-n} \left[1 - n \left(\frac{v}{\phi + V_e}\right) + \frac{n(n+1)}{2} \left(\frac{v}{\phi + V_e}\right)^2 + \ldots \right] \frac{dV}{dt} \qquad (A.14)$$

Current I consists of a fundamental as well as harmonic components. The voltage developed in $C(V)$ is found by solving for V as a function of Q. From equation (A.10) we have:

$$\phi + V = \left[\frac{(1 - n)\, Q}{C_{min} (\phi + V_B)^n} \right]^{\frac{1}{1-n}} \qquad (A.15)$$

When an a.c. charge q is superimposed on a fixed d.c. charge Q_o at the bias voltage V_e, equation (A.15) becomes:

$$\phi + V = V_o \left[\frac{(1 - n)\, Q}{C_{min} (\phi + V_B)^n (\phi + V_e)^{1-n}} \right]^{\frac{1}{1-n}} \qquad (A.16)$$

where $V_o = \phi + V_e$

Equation (A.16) can be written in a more convenient form as:

$$\phi + V = V_o \left[\frac{Q}{Q_o}\right]^{\frac{1}{1-n}}$$

$$= V_o \left[\frac{Q_o + q}{Q_o} \right]^{\frac{1}{1-n}} = V_1 \left[1 + \frac{q}{Q_o} \right]^{\frac{1}{1-n}} \qquad (A.17)$$

where

$$Q_o = \frac{C_{min} (\phi + V_B)^n (V_o)^{1-n}}{1 - n} \qquad (A.18)$$

Expanding equation (A. 17) into a binomial series we have:

$$\phi + V = V_o[\, 1 + \frac{1}{1-n} (\frac{q}{Q_o}) + \frac{(\frac{1}{1-n}) (\frac{1}{1-n} - 1)}{2} (\frac{q}{Q_o})^2 \ldots] \qquad (A.19)$$

Again the voltage across the non-linear capacitance contains fundamental as well as harmonic components. Making the small signal approximation and taking the value of $n = \frac{1}{2}$ for abrupt junction case we have:

$$\phi + V = V_o[1 + 2(\frac{q}{Q_o}) + (\frac{q}{Q_o})^2] \qquad (A.20)$$

The d.c. operating charge Q_o may be approximated by

$$Q_o \simeq \frac{C_{min} V_B}{1-n} \qquad (A.21)$$

where ϕ has been neglected in comparison to V_B and $V_B \simeq V_e$.

To show how the non-linear capacitance varies with time we re-write (A. 4) for a superimposed a.c. bias, i.e.

$$C = \frac{K}{[V_e + v]^{1/2}} \qquad (A.22)$$

Since $v = V \cos \omega t$ (the applied a.c. voltage) we have:

$$C = \frac{K^{1/2}}{[V_e]} \frac{1}{[1 + a \cos \omega t]^{1/2}} \tag{A.23}$$

where: $a = \frac{v}{V_e}$

we now have a non-linear capacitance which is a periodic function of time and can be represented by a fourier series expansion of the form

$$C(t) = \sum_{n=0}^{\infty} C_n \cos n \omega t \tag{A.24}$$

where

$$C_n = C(V_e) \left[\frac{1}{\pi} \int_{-\pi}^{+\pi} \frac{\cos n\omega t}{1 + a \cos \omega t} \right]^{1/2} d\omega t \tag{A.25}$$

$$C(V_e) = \frac{K}{[V_e]}^{1/2}$$

APPENDIX B

VARACTOR DOUBLER ANALYSIS

B.1 DOUBLER EQUATIONS OF MOTION:

B.1.1 General

In this appendix we present the analysis for the varactor frequency doubler based on the idealized circuit shown in Figure (3.4). Analysis of an idealized circuit such as this will yield equations characteristic of the varactor only. In practical applications the effects of non-ideal circuits must, of course, be taken into account.

Extensive literature on the analysis of frequency multipliers has been presented by Utsunomya and Yuan [36], Johnson [37], and others [38]. However, most of these analyses are restricted to specific circuit conditions, deal with lossless varactor models or with doublers only, or use small signal Taylor expansions. To date, the most comprehensive analysis of frequency multipliers is presented by Penfield and Rafuse [39]; a brief outline of the theory developed by them will be presented here. The lossy Uhlir varactor model of Figure (2.2C) leads to the following varactor equation:

$$e(t) = R_s i(t) + \int S(t)\, i(t)\, dt \quad \text{(neglecting noise)} \qquad (B.1)$$

where $s(t)$ is the incremental time varying elastance.

Since in harmonic multipliers, all frequencies are harmonically related, it is convenient to express the charge, current, voltage and elastance in terms of Fourier series [40] as follows:

$$q(t) = \sum_k Q_k \exp j\, k\omega_o t \tag{B.2}$$

$$i(t) = \sum_k I_k \exp j\, k\, \omega_o t = \sum_k Jk\, \omega_o\, Q_k \exp Jk\, \omega_o t \tag{B.3}$$

$$v(t) = \sum_k V_k \exp jk\, \omega_o t \tag{B.4}$$

$$e(t) = \sum_k E_k \exp jk\, \omega_o t \tag{B.5}$$

$$s(t) = \sum_k S_k \exp jk\, \omega_o t \tag{B.6}$$

where the sum extends from $k = -\infty$ to $+\infty$, and where, because $V(t)$, $i(t)$, and $s(t)$ are real $Q_{-k} = Q_k^*$, $I_{-k} = I_k^*$, $V_{-k} = V_k^*$, $E_{-k} = E_k^*$ and $S_{-k} = S_k^*$. Further useful definitions which will be used later are the modulation ratios, cutoff frequency.

The modulation ratio is definted as:

$$m_k = \frac{|\, S_k \,|}{S_{max} - S_{min}} \tag{B.7}$$

The cutoff frequency is defined as:

$$w_c = \frac{S_{max} - S_{min}}{R_s} \tag{B.8}$$

From Equation (B.1) each Fourier coefficient E_k can be expressed in terms of the Fourier coefficients of the current and elastance. The Fourier coefficients for a periodic function with a period normalized to

unity†, may be expressed as: (Papoulis [36]),

$$E_k = \int_0^1 [e(t) \exp - 2\pi j\ k\ t]\, dt \qquad (B.9)$$

By substituting (B.9) into (B.1) we have

$$E_k = R_s\ I_k + \frac{1}{2\pi j k} \sum_n I_n\ S_{k-n} \qquad (B.10)$$

Since current is allowed to flow at only the fundamental and second harmonic frequency, the only I_n present are those for $n = -2, -1, 1$ and 2, and the only S_{k-n} present are those for $k - n = -2, -1, 0, 1$ and 2.

i.e. $$E_1 = (R_s + \frac{S_o}{2\pi j})\ I_f + \frac{S_2\ I_f^*}{2\pi j} + \frac{S_1 I_{2f}}{2\pi j} \qquad (B.11)$$

and $$E_3 = (R_s + \frac{S_o}{2\pi j2})\ I_{2f} + (\frac{S_1}{4\pi j 2})\ I_f \qquad (B.12)$$

Since in the case of abrupt junction varactors, the elastance charge relationship is linear,

$$\frac{S_1}{S_2} = \frac{2\ I_f}{I_{2f}} \quad ; \quad \frac{S_1^*}{S_2} = \frac{-\ 2\ I_f^*}{I_{2f}}$$

---

† $w = (2\pi)(1) = 2\pi$. It is considered convenient to normalize the frequency to unity here. Any other frequency may be used in (B.1) and the equations to follow.

hence (B.11) and (B.12) become;

$$E_1 = (R_s + \frac{S_o}{2\pi j}) I_f + \frac{S_1^* I_{2f}}{2\pi j 2} \qquad (B.13)$$

$$E_2 = (R_s + \frac{S_o}{2\pi j 2}) I_{2f} + \frac{S_1^2}{4 S_2 2\pi j} \qquad (B.14)$$

B.1.2 Output Impedance

According to Figure (3.4) the output impedance is given by

$$Z_L = - \frac{E_2}{I_{2f}} \qquad (B.15)$$

where output impedance Z_L can be said to be complex consisting of $R_L = k X_L$.

Substituting (B.15) into (B.14)

$$(Z_L + R_s + \frac{S_o}{2\pi J 2}) = \frac{-S_1^2}{4 S_2 2\pi j} \qquad (B.16)$$

The quantity $(Z_L + R_s + \frac{S_o}{2\pi J 2})$ may be represented on a complex plane with magnitude $(Z_L + R_s \frac{S_o}{2\pi j 2})$ and phase angle θ

$$Z_L + R_s + \frac{S_o}{2\pi j 2} = \frac{R_L + R_s}{\cos \theta} \exp J \theta \qquad (B.17)$$

By using (B.7), (B.8), (B.15), and (B.17) an expression for the output resistance results;

$$R_L = R_s (\frac{m_1^2}{2 m_2} \frac{C}{2} \cos \theta - 1) \qquad (B.18)$$

where $C = \frac{\omega_c}{\omega_o}$, ω_o is the fundamental radian frequency. Now from (B.17) and (B.18)

$$Z_L = - R_s - \frac{S_o}{2\pi j 2} + R_s \frac{m_1^2}{2 m_2} \frac{C}{2} \exp j\theta \qquad (B.19)$$

B.1.3 Input Impedance

By combining (B.13), (B.17), (B.18), it is found that,

$$E_1 = Z_{in} I_f \qquad (B.20)$$

where $$Z_{in} = R_s + \frac{S_o}{2\pi j} + R_s \frac{C}{2} 2 m_2 \exp - j\theta \qquad (B.21)$$

$$(\text{Real}) Z_{in} = R_{in} = R_s (1 + 2 m_2 \frac{C}{2} \cos\theta) \qquad (B.22)$$

B.1.4 Input Power

The input power may be written in terms of the input current and resistance as follows:

$$P_{in} = 2 \left| I_f \right|^2 R_{in} \qquad (B.23)$$

The maximum varactor diode is V_B, and at breakdown the charge is Q_B and elastance S_{max}. The minimum varactor voltage is V_{min} and at this minimum voltage the charge is Q_{min} and the elastance S_{min}. From linear relationship betweeen charge and elastance

$$\frac{S - S_{min}}{S_{max} - S_{min}} = \frac{q - Q_{min}}{Q_B - Q_{min}} \qquad (B.24)$$

also $$Q_B - Q_{min} = \frac{2(V_B - V_{min})}{S_{max} + S_{min}} \qquad (B.25)$$

The Fourier coefficient I_f may be extracted from (B.3).

As $I_f = 2\,j\pi Q_1$ and from (B.24) and (B.7) one can write

$$I_f = 2\pi j\, m_1 (Q_B - Q_{min}) \qquad (B.26)$$

Now by using (B.25), (B.7), (B.8), (B.25), (B.23) and the expression: $P_{normal} = \frac{(V_B + \phi)^2}{R_S}$, it can be shown by mere subsitution that

$$P_{in} = 2\,P_{norm} \left(\frac{S_{max} - S_{min}}{S_{max} - S_{min}}\right)^2 \left(\frac{2}{C}\right)^2 m_1^2 \left(1 + 2\,m_2 \frac{C}{2} \cos\theta\right) \qquad (B.27)$$

B.1.5 Output Power

The output power can be represented by a similar expression, $P_{out} = 2\,|\,I_{2f}\,|^2\,R_L$, which results in the equation

$$8\,P_{norm} \left(\frac{S_{max} - S_{min}}{S_{max} + S_{min}}\right)^2 \left(\frac{2}{C}\right)^2 m_2^2 \left(\frac{m_1^2}{2m_2} \frac{C}{2} \cos\theta - 1\right) \qquad (B.28)$$

B.1.6 Efficiency

The conversion efficiency is obtained simply by taking the ratio

$$\varepsilon = \frac{P_{out}}{P_{in}} = \frac{\frac{C}{2}\cos\theta - \frac{2m_2}{m_1^2}}{\frac{C}{2}\cos\theta + \frac{1}{2m_2}} \qquad (B.29)$$

b.1.7 Summary of Doubler Equations

Considerable simplification of the doubler formulae is achieved by assuming that the angle θ is zero (i.e. tuned out in the circuit). Values for R_{in}, R_L, P_{in}, P_{out}, and ε are easily obtained if m_1 and m_2 are known. However, solutions of m_1 and m_2 in terms of these parameters cannot readily be obtained. Iterative numerical techniques are tedious and usually require the aid of a computer. Penfield and Rafuse [39] resorted to a graphical inversion technique which shows various compatible operating conditions, relating the parameters of interest. The author has deduced values of m_1 and m_2 from these plots for $C = 15$. These are

$$m_1 = 0.250$$

$$m_2 = 0.117$$

Using these values of m_1 and m_2, and also $\theta = 0$, the doubler formulae become

$$R_{in} \simeq R_s$$

$$R_2 \simeq R_s$$

$$P_{in} \simeq 0.5\ P_{norm} \left(\frac{\omega_o}{\omega_c}\right)^2 \qquad (B.30)$$

$$P_{out} \simeq 0.002\ P_{norm} \qquad (B.31)$$

$$= 0.004 \left(\frac{\omega_c}{\omega_o}\right)^2 \qquad (B.32)$$

A plot of ε vs $\frac{\omega_c}{\omega_o}$ and $\frac{P_{in}}{P_{normal}}$ vs $\frac{\omega_o}{\omega_c}$ is given in Figures (B.1) and (B.2) respectively.

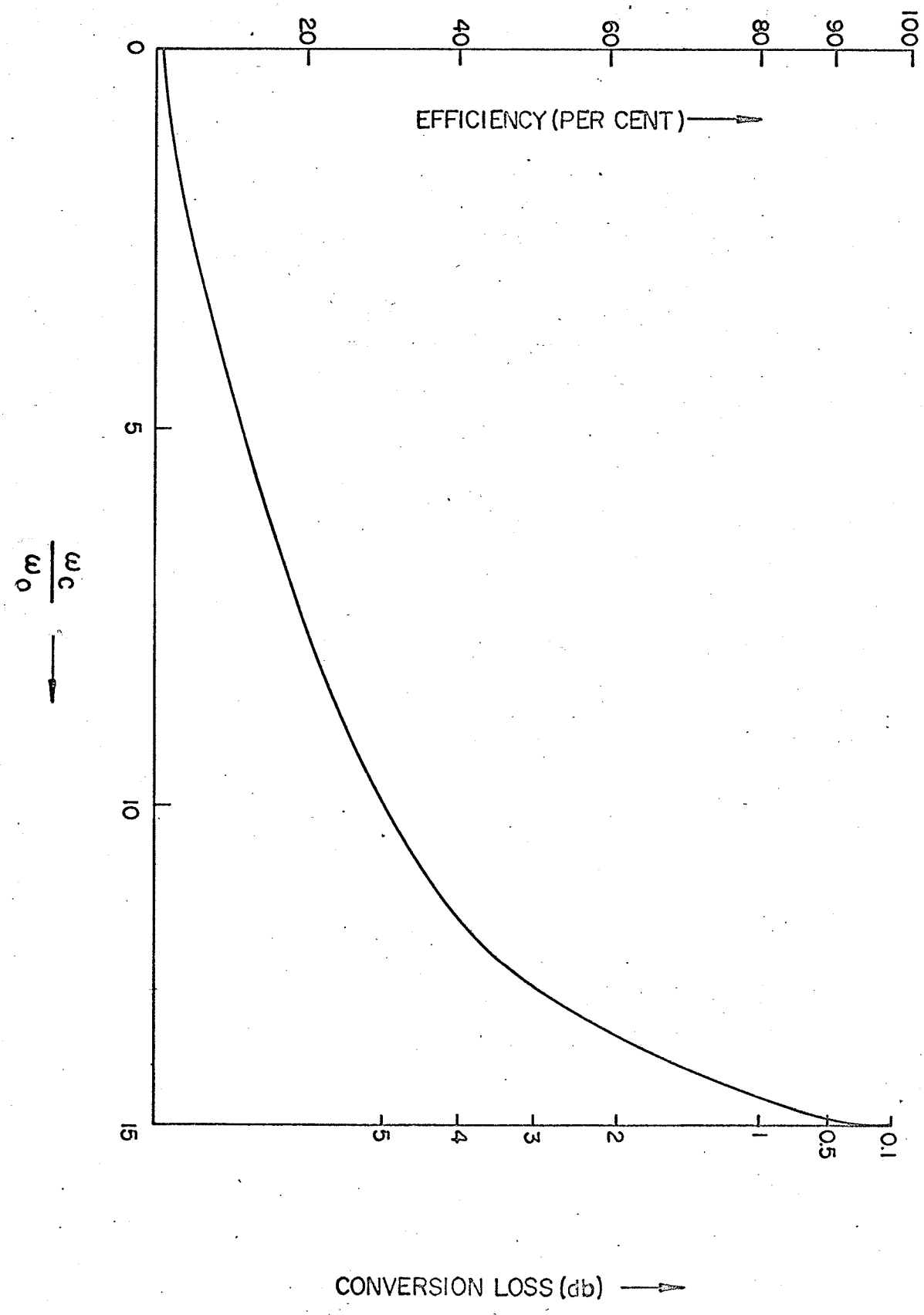
EFFICIENCY (PER CENT)
0
20
40
60
80
90
100
5
10
15
$\frac{\omega_c}{\omega_0}$
5
4
3
2
1
0.5
0.1
CONVERSION LOSS (db)

fig.B.1

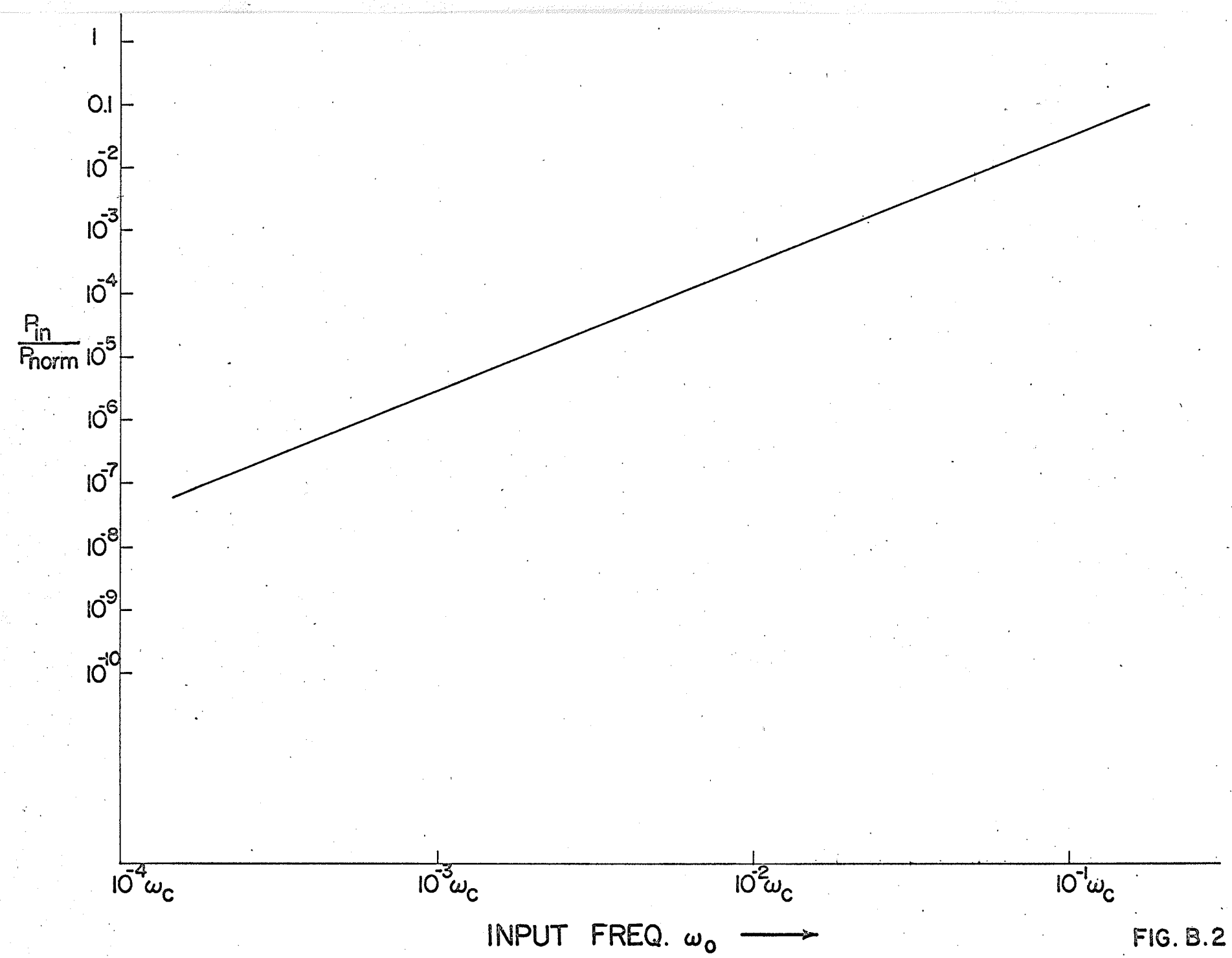
1
0.1
10^{-2}
10^{-3}
10^{-4}
10^{-5}
10^{-6}
10^{-7}
10^{-8}
10^{-9}
10^{-10}
$\frac{P_{in}}{P_{norm}}$
$10^{-4}\omega_c$
$10^{-3}\omega_c$
$10^{-2}\omega_c$
$10^{-1}\omega_c$
INPUT FREQ. ω_0 ⟶

FIG. B.2

APPENDIX C

THE DESIGN OF WAVEGUIDE BAND-PASS FILTER

The band-pass filter designed here, corresponds to direct-coupled filter using small irises, and is used to extract the second harmonic frequency from the harmonic generator. The design of a cavity resonator filter coupled by small irises can be carried out in a general fashion by means of Bethe's small aperture theory [42]. Figure (C.1) shows an arrangement used for the construction of the filter. This is a three-resonator filter designed for a 1.0 percent bandwidth, maximally flat response centered at 9 GHz. The resonators are coupled by two rectangular irises at the ends and two circular irises in the middle as shown in the Figure (C.1). The lumped equivalent circuit of the above band pass filter is also shown in the Figure.

DESIGN CALCULATIONS:

The dimensions of the waveguide are:

a = 0.9 inches

b = 0.4 inches.

center frequency f_o = 9 GHz

fractional band-width ω = 1%

For narrow-band filters, the low-pass to band-pass mapping [43] is given by:

$$\frac{\omega'}{\omega_1'} = \frac{2}{\omega}\left(\frac{f - f_o}{f_o}\right)$$

where

$$\omega = \frac{\omega_2 - \omega_1}{\omega_o}$$

and

$$\omega_o = \frac{\omega_2 + \omega_1}{2}$$

ω' and ω_1' refer to the low-pass filter response as discussed in [44], while ω_1 and ω_2 are the lower and the upper side band frequencies for the band-pass filter.

Hence upper side-band frequency - 9.05 GHz

and lower side-band frequency = 8.95 GHz

guide wavelength λ_g at 9 GHz = 4.063 cms

we choose $\ell = \lambda_g/2 = \frac{4.863}{2} = 0.95$ inches

The elements of the low-pass prototype filter are determined from Table 4.05-1(a) in [44] to be

$$g_o = g_4 = 1.000$$

$$g_1 = g_3 = 1.000$$

$$g_2 = 2.000$$

We determine from Figure 8.02-3 [44] that external Q is given by:

$$(Q_e)_A = (Q_e)_B = g_o\, g_1\, \frac{\omega_1'}{\omega}$$

$$= \frac{1}{.01} = 100$$

and

$$K_{12} = K_{23} = \frac{\omega}{(\omega_1' = g_1\ g_2)} = \frac{.01}{2} = \frac{.01}{1.414} = 0.007$$

using Figures 8.07-1(a) and 8.07-2(a) in [44] we find the polarizabilities M_1 for the external and internal apertures to be:

$$Q_e = \frac{\ell^3\ a^2\ b^2\ \lambda g}{4\pi\ M_1^2\ \lambda^2} \quad (S = 1)$$

$$100 = \frac{(0.95)^3 \times (0.9)^2\ (0.4)^2 \times 1.90}{4 \times 3.14 \times M_1^2 \times (1.31)^2}$$

Hence $M_1 = \underline{8 \times 10^{-3}}$ for the external aperture.

For the internal aperture we have:

$$K = \frac{M_1\ \lambda^2}{\ell^3\ ab}$$

Hence

$$M_1 = \frac{0.007 \times (0.95)^3 \times 0.9 \times 0.4}{1.71}$$

$$= \underline{1.25 \times 10^{-3}}$$

For the rectangular iris we choose

$$\frac{d_2}{d_1} = 0.5$$

Referring to Figure 5.10-4(a) in [44] we find from the curve for rectangular irises the value of d_1 to be:

$$\frac{M_1}{d_1^3} = 0.152$$

Hence $d_1 = 0.37$ inches

and therefore $d_2 = 0.5 \times .37 = 0.185$ inches

After applying the correction as given in [45]., i.e.

$$M_1' = \frac{M_1}{1 - (\frac{\lambda_c}{\lambda})^2}$$

we obtain

$$d_1 = \underline{0.355 \text{ inches}}$$

$$d_2 = \underline{0.177 \text{ inches}}$$

For the circular middle irises we find

$$d = (6M_1)^{1/3}$$

$$= (6 \times 1.25 \times 10^{-3})^{1/3}$$

$$= \underline{0.195 \text{ inches}}.$$

Three tuning screws were placed at the centers of the cavities for fine tuning at 9 GHz.

IRIS COUPLED WAVEGUIDE BAND-PASS FILTER

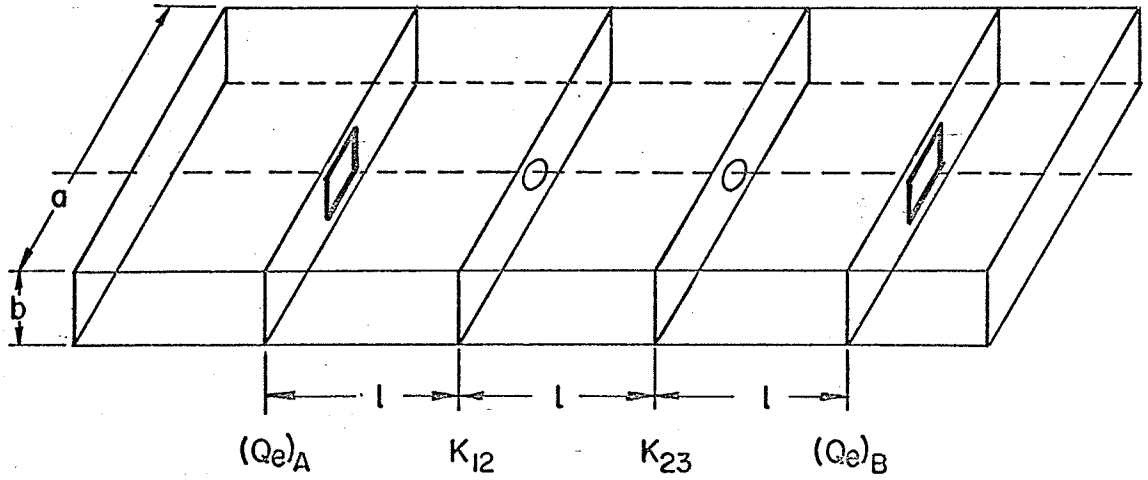

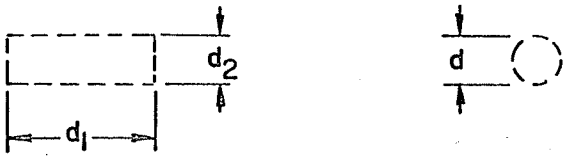

DIMENSIONS OF THE IRISES

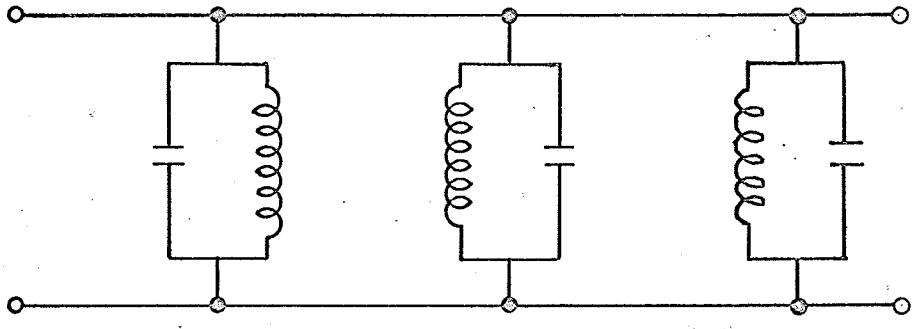

LUMPED EQUIVALENT CIRCUIT

FIGURE (C.1)

REFERENCES

[1] R. J. Bauer, M. Coh, J. M. Cotton, Jr., and R. F. Packard, "Millimeter Wave Semiconductor Diode Detector, Mixers and Frequency Multipliers", Proc. IEEE, Vol. 54, pp. 595-605, April 1966.

[2] L. E. Dickens, "Millimeter Wave Diodes for Harmonic Power Generation", IEEE Trans. on Microwave Theory and Techniques, vol. MTT-15, No. 1, pp. 32 - 37, January 1967.

[3] Fifth International Electronics Show, Paris, reported in Electronics, p. 40, March 16, 1962.

[4] W. W. Teich, "New Approaches to Millimeter Wavelengths Devices", Electronics, pp. 37 - 44, May 25, 1962.

[5] J. R. Pierce, "Millimeter Waves", Phys. Today, vol. 3, pp. 24 - 29, November 1950.

[6] W. E. Hughes, "Maser Operation at 96 GHz with Pump at 65 GHz", Proc. IEEE, vol. 50, p. 1691, July 1962.

[7] W. C. King, and W. Gordy, "One to Two Millimeter Wave Spectroscopy", Phys. Rev., vol. 90, pp. 319 - 320; April 1953.

[8] C. H. Page, "Frequency Conversion with Positive Non-linear Resistors", J. Res. NBS, vo. 56, pp. 179 - 182, April 1956.

[9] J. M. Manley and H. E. Rowe, "Some General Properties of Non-linear Elements - Part I General Energy Relations", Proc. IRE, vol. 44, pp. 904 - 913, July 1956.

[10] A. Uhlir, Jr., "The potential of Semiconductor Diodes in High Frequency Communications", Proc. IRE, vol. 46, pp. 1099 - 115, June 1958.

REFERENCES (continued)

[11] A. E. Bakanowski, N. G. Cranna and A. Uhlir, "Diffused Silicon non Linear Capacitors", IRE Trans. on PGED, Jan. 5, 1959.

[12] M. Wenohara, "An Extremely Low Noise Nondegenerate Parametric Amplifier", Proc. IRE, vol,50, no. 2(L), 1962.

[13] N. Houlding, "Low Noise Parametric Amplifier", Proc. IRE, vol. 47, No. 11 (L), 1959.

[14] R. C. Knechtli, and R. D. Weglein, "Low Noise Parametric Amplifier", Proc.IEEE, Vol. 48, no. 7, 1960.

[15] W. Schockly, "The Theory of P-N Junctions in Semiconductors", Bell Syst. Tech. Journal, vol. 28, p. 435, 1949.

[16] H. C. Torrey and C. A. Whitmer, "Crystal Rectifiers", M.I.T. Rad, Lab,Ser., vol. 15, New York; McGraw-Hill, 1948, pp. 68 - 107.

[17] D. Dewitt and A. L. Rossoff, "Transistor electronics", McGraw-Hill, 1957, pp. 57 - 74.

[18] A. Uhlir, Jr., op cit.

[19] S. P. Morgan, and F. M. Smits, "Potential Distribution and Capacitance of a Graded p-n Junction", Bell System Tech. J., vol. 39, pp 1573 - 1602, November 1960.

[20] Fred Sterzer, "Microwave Parametric Subharmonic Oscillators for Digital Computing", Proc. IRE, Vol. 47, no. 8, 1959.

[21] K. K. N. Chang, "Harmonic Generation with Non-linear Reactances", RCA Review, vol. 19, no. 3, p. 455, 1958.

[22] R. L. Rulison and C. H. Bricker, "Varactor Frequency Doubler From 11.5 GHz to 23 GHz", Proc.IEEE, Vol. 50, No. 12(L), 1962.

REFERENCES (continued)

[23] T. M. Hytlin, and K. L. Katzebue, "A Solid State Microwave Source from Reactance-diode Harmonic Generators", IRE Trans. on Microwave theory and Techniques, vol. MTT-9, pp. 73-78, January 1961.

[24] J. Hilibrand and W. R. Beam, "Semiconductor Diodes in Parametric Subharmonic Oscillators", RCA Rev. vol. 20, pp. 229 - 253, June 1959.

[25] E. S. Kuh, "Theory and Design of Wide-band Parametric Converters", Proc.IEEE, vol. 50, pp. 31 - 38, January 1962.

[26] B. C. DeLoch, "17.35 and 30 GHz Parametric Amplifiers", Proc. IRE, vol. 48, p. 1323, July 1960.

[27] C. A. Burrus, "Formed-Point Contact Varactor Diodes Utilizing a Thin Expitaxial Gallium Arsenide Layer", Proc.IEEE, vol. 51, pp. 1777 - 1778, December 1963.

[28] T. Moreno, "Microwave Transmission Design Data", McGraw-Hill Book Co. Inc., N.Y., 1948, p. 154.

[29] W. J. Getsinger, "Mounted Diodes", IEEE Trans. on Microwave Theory and Techniques, vol. MTT-14, p. 58, Feb. 1966.

[30] Steele, K. A. "Broadband Harmonic Generator Converts from s-Band to x-Band". Canadian Electronic Engineering, vol. 3, No. 7, July 1959, pp. 26 - 28.

[31] Ragan, George L., "Microwave Transmission Circuits", Mass. Inst. of Technology, Radiational Laboratory Series, vol. 9, McGraw-Hill Book Co. Inc., N.Y., 1948, p. 100 - 114.

[32] D. Parker, "Increased Power Handling Capability and Improved Efficiency of Frequency Multipliers Using Varactor Arrays", Proc. on Engineering Applications and Electronic Phenomenon. Aug. 1967, pp. 378 - 395.

REFERENCES (continued)

[33] Lee, H. C., and Robert Minton, "Designing Transistor Multipliers", Microwaves, vol. 4, no. 11, Nov. 1965, pp. 18 - 28.

[34] M. Krakauer, "Harmonic Generation with Step Recovery Diodes", Proc.IEEE, vol. 50, no. 7, July 1962, pp. 1665 - 1676.

[35] K. K. N. Chang, "Parametric and Tunnel Diodes", Prentice-Hall Inc., N.J., 1964, p. 25.

[36] U. T. Sunamiya and S. Yuan, "Theory, Design and Performance of Maximum Efficiency Variable-Reactance Multipliers", Proc. IEEE, vol. 50, no. 1, Jan. 1962, pp. 57 - 65.

[37] K. M. Johnson, "Large Signal Analysis of a Parametric Harmonic Generator", Trans.IEEE, vol. MTT - 8, no. 5, Sept. 1961, pp. 525 - 532.

[38] K. K. N. Chang, "Harmonic Generation with Nonlinear Reactances", RCA Rev., vol. 19, pp. 455 - 464, Sept. 1958.

[39] P. Penfield, and R. P. Rafuse, "Varactor Applications", MIT Press, Cambridge, Mass., 1962.

[40] A. Papoulis, "The Fourier Integral and its Applications", McGraw-Hill Book Co. Inc., N.Y. 1962.

[41] Uhler, A. Jr., "Similarity Considerations for Varactor Multipliers", Microwave Jnl., vol. 5, no. 7, July 1962, pp. 55 - 59.

[42] H. A. Bethe, "Theory of Side Windows in Waveguides", Report 43-27, M.I.T. Rad. Lab., Cambridge, Mass. April 1943.

[43] Matthaei, Young and Jones, "Mcirowave Filters, Impedance Matching Networks, and Coupling Structures", McGraw-Hill, N.Y. 1964, p. 462.

REFERENCES (continued)

[44] Matthaei, Young and Jones, op. cit. p. 428.

[45] Matthaei, Young and Jones, op. cit. p. 242.

[46] Eng, Sverre T. "Characterization of Microwave Variable Capacitance Diodes", IEEE Transactions on Microwave Theory and Techniques, Vol. MTT-9, No. 1, January 1961, pp. 11 - 22.

[47] K. D. Froome, "Microwave Harmonic Generator Capable of Frequencies in Excess of 600 GHz", Nature, vol. 193, pp. 1169 - 70, March 24, 1962.